

1      **Bacterial cell numbers and community structures of seawater biofilms depend on the**  
2                                      **attachment substratum**

3                                      Scott A. Yap <sup>1</sup>, Giantommaso Scarascia <sup>1</sup>, Pei-Ying Hong <sup>1</sup>

4      <sup>1</sup> King Abdullah University of Science and Technology (KAUST), Water Desalination and Reuse Center  
5                                      (WDRC), Biological and Environmental Science & Engineering

6                                      Division (BESE), Thuwal, 23955-6900, Saudi Arabia  
7  
8  
9

10    \* **Corresponding author:**

11    Pei-Ying Hong

12    Email: [peiying.hong@kaust.edu.sa](mailto:peiying.hong@kaust.edu.sa)

13    Phone: +966-12-8082218  
14

15    **Contact details of co-authors:**

16    Scott A. Yap:

17    Email: [scott.yap@kaust.edu.sa](mailto:scott.yap@kaust.edu.sa)  
18

19    Giantommaso Scarascia:

20    Email: [giantommaso.scarascia@kaust.edu.sa](mailto:giantommaso.scarascia@kaust.edu.sa)  
21  
22

23    **Keywords:** Biofouling, biocorrosion, titanium, stainless steel, polyethylene, polycarbonate, sulfate-  
24    reducing bacteria

25    **Running title:** Seawater biofilm on plastic and metal surfaces  
26

27 **Abstract**

28 Seawater is increasingly being used as a source for various industrial applications. For such  
29 applications, biofilm growth creates various problems including but not limited to pipe  
30 biocorrosion. In this study, it is hypothesized that the material type is preferred by certain  
31 bacterial populations in the seawater to attach and establish biofilms. By comparing differences  
32 in the total cell counts and microbial communities attached to high density polyethylene (HDPE),  
33 polycarbonate, stainless steel (SS316) and titanium, the appropriate material can be used to  
34 minimize biofilm growth. All four materials have hydrophilic surfaces, but polycarbonate  
35 exhibits higher surface roughness. There were no significant differences in the cell numbers  
36 attached to polycarbonate, HDPE and titanium. Instead, there were significantly fewer cells  
37 attached to SS316. However, there was a higher relative abundance of genera associated with  
38 opportunistic pathogens on SS316. Copy numbers of genes representing Desulfobacteraceae and  
39 Desulfobulbaceae, both of which are sulfate-reducing bacteria (SRB), were approximately 10-  
40 fold higher in biofilms sampled from SS316. The enrichment of SRB in the biofilm associated  
41 with SS316 indicates that this material may be prone to biocorrosion. This study highlights the  
42 need for industries to consider the choice of material used in seawater applications to minimize  
43 microbial-associated problems.

44

## 45 **1. Introduction**

46           Seawater is increasingly being used as a source for various industrial applications in an  
47 attempt to alleviate the demand for freshwater. Examples of such industrial applications include  
48 seawater cooling tower systems and seawater injection for enhanced oil recovery. In most  
49 instances, seawater is usually recirculated at least once to minimize operating costs associated  
50 with continuous pumping of new seawater into the system. However, recirculating seawater  
51 allows for microbes, minerals and nutrients to accumulate within the system [1]. To tackle  
52 inorganic scaling problems arising from minerals, antiscalants are commonly used even though  
53 they generally include components of polymers, phosphates and phosphonates and can contribute  
54 nutrients that support microbial growth [2]. Hence, extensive biofilm growth is an inevitable  
55 problem in seawater pipelines.

56           Biofilm growth creates a suite of problems. For example, biofilms can serve as  
57 colonization platforms for pathogens to augment their environmental persistence [3, 4]. Biofilm  
58 formation is also correlated with the occurrence of biocorrosion [5], otherwise known as  
59 microbial-induced corrosion (MIC). This is shown by an increased rate of corrosion in the  
60 presence of biofilms [6]. Although total eradication of biofilms and the associated microbial  
61 populations would be impractical, efforts have been undertaken to minimize cell counts and  
62 bacterial populations that may be present in the biofilm by varying certain operational factors.  
63 These factors include maintaining the presence of residual disinfectant, optimizing water age,  
64 hydraulic regimes and pipe materials [7-15].

65           However, most of the existing studies utilized culture-based approaches or DNA-based  
66 fingerprinting techniques to determine potential impacts on the biofilm arising from these  
67 operational factors. Cultivation-based approaches to enumerating cell counts are subject to bias

68 and are not representative of bacterial species that are fastidious about growth conditions [16,  
69 17]. When compared to high-throughput amplicon-based sequencing approaches, fingerprinting  
70 techniques, including denaturing gel electrophoresis or terminal restriction length  
71 polymorphisms, are not able to provide an in-depth characterization of the bacterial community  
72 structure. Neither are the fingerprinting techniques capable of providing quantitative  
73 measurements of certain bacterial populations when compared to the quantitative PCR (qPCR)  
74 approach. An earlier study used high-throughput sequencing to show that bacterial and/or  
75 eukaryotic community structures in drinking water biofilms can be affected by these factors.  
76 Specifically, pipe materials only affect the bacterial community structure but not the eukaryotic  
77 community [8]. However, similar studies on the variation of cell counts and bacterial community  
78 structures in seawater in relation to the pipe materials are not widely available.

79         A better understanding of whether material types result in differences in microbial  
80 populations, specifically, sulfate-reducing bacteria (SRB) and genera associated with  
81 opportunistic pathogens, is needed to assess the potential relevance to industrial stakeholders and  
82 public health. SRB possess organic filaments similar to nanowires [18], which may play a role in  
83 adhesion, biofilm formation and direct interspecies electron transfer [19]. Adherence to a  
84 conductive material may facilitate extracellular electron transfer and metal reduction, both of  
85 which are key metabolic traits required by the SRB [20]. As such, SRB are generally thought to  
86 be the protagonist in biocorrosion [21]. Biocorrosion is believed to account for 20% of the  
87 damage caused by corrosion [22], which can impart a tremendous financial burden on industrial  
88 stakeholders. In addition, the presence of opportunistic pathogens can also pose potential health  
89 threats to certain groups of individuals, for example, immunocompromised patients, the elderly  
90 and infants, upon exposure.

91           In this study, it is hypothesized that the material type is preferred by certain bacterial  
92 populations in the seawater to attach and establish biofilms. It is further hypothesized that the  
93 type of material plays a less significant role in affecting the total cell count and composition of  
94 the microbial community as the biofilm ages. The materials tested were stainless steel 316 (i.e.,  
95 SS316), titanium, high density polyethylene (HDPE) and polycarbonate. SS316 and titanium are  
96 commonly used in the heat exchangers [23] for industrial seawater applications. HDPE and  
97 polycarbonate are included in this study to serve as non-metal controls and because they are  
98 plastic materials commonly used in industrial applications. Efforts were made to determine the  
99 effect of materials on the genera associated with opportunistic pathogens and sulfate-reducing  
100 bacteria (SRB). To address these issues, counts of cells adhering to the different type of materials  
101 were enumerated by flow cytometry, while both high-throughput sequencing and qPCR were  
102 utilized to characterize the microbial community structures.

103

## 104 **2. Materials and methods**

### 105 **2.1. Experimental procedure**

106 The materials tested in this study were stainless steel 316 (i.e., SS316), titanium, high density  
107 polyethylene (HDPE) and polycarbonate. These materials were characterized for their surface  
108 roughness and hydrophilicity as detailed in Section 2.2. The materials were then placed inside  
109 bioreactors and exposed to seawater over a period of four months (Section 2.3). Seawater biofilm  
110 established on the materials were harvested using sampling procedure described in Section 2.4.  
111 The harvested samples were divided into two portions. The first portion was determined for the  
112 total bacterial cell counts by flow cytometry (Section 2.5). The second portion was extracted for  
113 DNA (Section 2.6), and the DNA was used in two types of molecular-based analyses. The first  
114 molecular-based analysis was 16S rRNA gene amplicon sequencing to characterize the microbial  
115 community attached on the different materials (Section 2.7). The second molecular-based  
116 analysis was quantitative PCR (qPCR) to quantify for the copy numbers of *Acinetobacter*  
117 *baumannii* (Section 2.8), Desulfobacteraceae and Desulfobulbaceae (Section 2.9).

### 118 **2.2. Material surface characterization**

119 The materials tested in this study were purchased from Biosurface Technologies (Bozeman, MT,  
120 USA) in a circular disc coupon format, each with a diameter of approximately 1.2 cm. All the  
121 materials that were tested in this study were evaluated for their surface roughness and extent of  
122 hydrophobicity based on procedures described previously [24]. Briefly, atomic force microscopy  
123 (AFM) was used to characterize the surface topography of each material type based on the  
124 standard protocol defined by American Society of Mechanical Engineer (ASME) B46.1-2009.  
125 AFM imaging was performed using Bruker Dimension ICON equipment (Santa Barbara, CA,  
126 USA) in soft tap mode to scan images of 15  $\mu\text{m}$  width by 15  $\mu\text{m}$  length at three random locations

127 on each material type. The AFM images were analyzed on Pico Image Software (Keysight  
128 Technologies Inc., Santa Rosa, CA, USA). Specifically, surface roughness is represented as the  
129 root mean square (RMS) average of profile height deviations from the mean height observed for  
130 that particular material. A higher RMS value indicates more apparent surface peaks and valleys,  
131 thus representing a rougher surface. The contact angle was measured by an Easy Drop Shape  
132 Analyzer (Kruss, Hamburg, Germany) in static mode at ambient temperature. Ultra-pure water  
133 was used as the probing liquid, and the mean values were determined from three different  
134 independent specimens. Generally, if the contact angle is smaller than  $90^\circ$ , the solid surface is  
135 considered hydrophilic and vice versa [25].

### 136 **2.3. Biofilm reactor operation**

137 From February to June 2016, a total of four Communicable Disease Centre (CDC) bioreactors  
138 (BioSurface Technologies, Bozeman, MT, USA) were operated at  $28^\circ\text{C}$  and at a stirring rate of  
139 200 rpm in the KAUST Water Desalination and Reuse Center (WDRC) (Figure 1). Each  
140 bioreactor had eight coupon holders that could be fitted with a total of 24 coupons of the same  
141 material per reactor. Seawater fed into the bioreactors was sourced from the Red Sea through an  
142 approximately 1 km pipeline to the WDRC laboratory. The seawater tap was flushed for 10  
143 minutes prior to collection of seawater in a sterile 20 L carboy container. Thereafter, seawater  
144 from the same container was fed at a continuous rate of 1.3 mL per minute to each bioreactor and  
145 replaced with fresh seawater every 10 days. The hydraulic retention time of seawater within the  
146 bioreactor was 6.4 h. The bioreactors were periodically checked for the hydraulic retention time,  
147 stirring rate, temperature and flow rate so as to ensure that the operating conditions among all  
148 four reactors are kept similar. Two L of seawater that was to be fed into the reactors were  
149 collected each month during the course of the experiment and evaluated for its total cell counts

150 and microbial community in accordance with protocols mentioned in the following subsections.  
151 All the bioreactors were covered with aluminum foil to limit exposure to light.

#### 152 **2.4. Sampling procedure**

153 Biofilm was sampled at 1 through 4 months after the commencement of the bioreactors. Six  
154 coupons for each type of material were collected during each sampling month and provided two  
155 sets of biological replicates for that particular sampling month. Each biological replicate  
156 comprised the pooled biomass scraped down from three coupons. The six coupons were selected  
157 from two coupon holders placed at random locations within the bioreactor to minimize any  
158 sampling bias due to the location of the coupon. New holders containing coupons of the same  
159 material type were replaced after each sampling event to ensure that the shear force was kept  
160 constant within the bioreactor. The sampled coupons were placed into separate petri dishes, and  
161 5 mL of 1X phosphate-buffered saline (PBS) solution was added. Autoclaved cotton swabs were  
162 then used to scrape down the loosely attached biofilm into the 1X PBS. The resulting suspension  
163 for each material was transferred to sterile 50 mL centrifuge tubes. The used cotton swabs and  
164 coupons were placed in a sterile centrifuge tube that contained 10 mL of 1X PBS. This tube was  
165 vortexed at high speed for 10 minutes with the aim of dislodging any attached biofilm on the  
166 cotton swab and coupons. Following this, the supernatant from each vortexed tube was  
167 transferred to the corresponding tube containing the loosely attached biofilm. A 20  $\mu$ L sample of  
168 the combined supernatant was set aside for total cell enumeration by flow cytometry. The  
169 remaining supernatant was centrifuged at 8000 g for 10 minutes, and the cell pellet was used for  
170 DNA extraction.

#### 171 **2.5. Flow cytometry to obtain total cell counts**



172 A 7  $\mu$ L sample of the supernatant or seawater was diluted 100-fold with 1X PBS, and 10  $\mu$ L of  
173 500 mM ethylenediaminetetraacetic acid (EDTA) was added to chelate metals and other  
174 inhibitors that can affect flow cytometry measurements. The mixture was briefly vortexed and  
175 incubated at 35 °C for 20 minutes. Then, 7  $\mu$ L of 100X SYBR Green I (Thermo Fisher Scientific,  
176 Carlsbad, CA, USA) was added, and the samples were incubated for 10 minutes. The number of  
177 cells in the resultant mixture was then quantified using a BD Accuri C6 (Thermo Fisher  
178 Scientific, Carlsbad, CA, USA) flow cytometer, based on protocol described by manufacturer  
179 [26].

## 180 **2.6. DNA extraction**

181 The microbial DNA from the biofilms was extracted using the UltraClean® PowerSoil DNA  
182 Isolation kit following the manufacturer's protocol with brief modifications as described  
183 previously [27]. To extract DNA from seawater, 2 L of seawater was first filtered through a 0.22  
184  $\mu$ m polycarbonate membrane filter (VWR, Radnor, PA, USA), and the retained biomass on the  
185 filter was extracted using a protocol similar to the one mentioned previously. The DNA  
186 concentration was then quantified using the Qubit Broad Range DNA Assay according to the  
187 manufacturer's protocol. The DNA was used for molecular-based analyses detailed in Section  
188 2.7 to 2.9.

## 189 **2.7. 16S rRNA gene-based amplicon sequencing and amplicon sequencing data analysis**

190 16S rRNA genes were amplified from the DNA with primer pair 515F and 907R based on  
191 procedures described earlier [24]. Purified amplicons were pooled and submitted to the KAUST  
192 Genomics Core lab for sequencing on the Illumina MiSeq platform. All high-throughput  
193 sequencing data were deposited in European Nucleotide Archive under accession number

194 PRJEB20120. The two main hypotheses of this study are that first, certain bacterial populations  
195 in the seawater prefer to attach to specific types of material prior to biofilm formation, and  
196 second, the type of material plays a less significant role in affecting the total cell count and  
197 composition of the microbial community as the biofilm ages. Amplicon sequences that denote  
198 the microbial community were therefore analyzed to test these two hypotheses. Sequences were  
199 sorted by the Bioinformatics Team at KAUST based on a Phred score of > 20. The sorted  
200 sequences were then trimmed off for the primers, barcodes and adaptor sequences, and any  
201 sequences > 300 nt in length were removed. Chimeras were identified and removed on UCHIME  
202 [28] by comparison with a core reference FASTA file downloaded from Greengenes  
203 (<http://greengenes.lbl.gov/Download/>). Chimera-free sequences were assigned to  
204 bacterial/archaeal taxonomic hierarchy at the 95% classification reliability level using the  
205 Ribosomal Database Project (RDP) Classifier [29]. The relative abundances of the bacterial and  
206 archaeal genera were calculated, collated and then square-root transformed. Square-root  
207 transformation was performed to down-weight the dominant taxa and to achieve a better balance  
208 of the abundant and rare species that are present in the samples. This allows the rare species,  
209 which are common in the data generated from high-throughput sequencing, to exert some  
210 influence on the calculation of similarity. The transformed data sets were then computed for their  
211 Bray–Curtis similarities and represented graphically for relative differences in bacterial  
212 community composition among samples aligned against either the materials or the duration of  
213 operation as factors in a boot-strapped metric multidimensional scaling (mMDS) plot. That is,  
214 samples that were further apart from each other shared less similarity than those that were closer  
215 together. All mMDS plots were obtained using Primer-E version 7 [30]. Chimera-free sequences  
216 were also submitted to the RDP pipeline for clustering analysis to identify the number of unique

217 operational taxonomic units (OTUs) with < 97% sequence similarity at each respective  
218 sequencing depth [31]. The number of unique OTUs identified at a sequencing depth of 2715  
219 sequences were collated and used to compare the level of microbial richness among the  
220 individual samples. This sequencing depth was used because this was the lowest number of reads  
221 obtained for one particular sample, and the comparison of the microbial richness across samples,  
222 therefore, had to be standardized at this depth.

## 223 **2.8. Quantitative PCR for *Acinetobacter baumannii***

224 *Acinetobacter baumannii* was chosen as the pathogenic bacterial species in the genus  
225 *Acinetobacter*, and its abundance was determined because this genus was detected in some of the  
226 biofilm samples. Copy numbers of the *ompA* gene representing *Acinetobacter baumannii* were  
227 determined using qPCR with a 7900 HT Applied Biosystems real-time PCR thermal cycler  
228 (Thermo Fisher Scientific, Carlsbad, CA, USA). Sequences of the primer pairs are listed in Table  
229 1. The qPCR standards were prepared as described previously [32, 33]. To produce qPCR  
230 standard curves, plasmid DNAs were diluted in series to form concentrations ranging from  $10^2$  to  
231  $10^8$  copies/ $\mu\text{L}$ . Each reaction volume of 20  $\mu\text{L}$  contained 10  $\mu\text{L}$  of Fast SYBR Green master mix,  
232 0.4  $\mu\text{L}$  of each primer (10  $\mu\text{M}$ ), 1  $\mu\text{L}$  of DNA template and 8.2  $\mu\text{L}$   $\text{H}_2\text{O}$ . The reaction for  
233 amplification was run using an annealing temperature of 60 °C, and the melting curve analysis  
234 was performed with a dissociation cycle which included an increment of temperature from 60 °C  
235 to 95 °C with intervals of 0.5 °C for 5 s each. The threshold cycle ( $C_q$ ) values for each dilution  
236 were plotted against the log-transformed concentration of each dilution. The amplification factor  
237 of the standards was 2.99, and the R-squared value was > 0.98. Amplifications to obtain standard  
238 curves were performed in triplicate, while test amplifications and negative non-template controls  
239 (NTCs) were run in duplicate. All NTCs had no determinable  $C_q$  values. The copy numbers

240 obtained from qPCR reactions were normalized against the total cell numbers obtained by flow  
241 cytometry for the corresponding sample.

## 242 **2.9. Quantitative PCR for SRB**

243 Both the Desulfobacteraceae and Desulfobulbaceae are families comprised of genera associated  
244 with SRB. The copy numbers of 16S rRNA genes representing total Desulfobacteraceae and  
245 Desulfobulbaceae were, therefore, determined to discern the presence and abundance of certain  
246 types of SRB. The qPCR standards for Desulfobacteraceae and Desulfobulbaceae were prepared  
247 by first amplifying the gene fragment with the appropriate primer pairs using DNA extracted  
248 from *Desulfobacter hydrogenophilus* DSM3380 and *Desulfobulbus elongatus* DSM2908 as  
249 bacterial templates. The amplified products were cloned into vectors, and the inserted genes were  
250 sequenced to verify that the sequences were perfectly complementary to the primer target region.  
251 The qPCR reactions were carried out as described above. The amplification factor of the  
252 standards ranged from 1.98 to 2.13 with R-squared values > 0.99. Amplifications to obtain  
253 standard curves were performed in triplicate, while test amplifications and NTCs were run in  
254 duplicate. All NTCs had no determinable C<sub>q</sub> values. Copy numbers obtained from qPCR were  
255 normalized against the total cell numbers obtained by flow cytometry for the corresponding  
256 sample.

## 257 **2.10. Statistical analyses**

258 Two-tailed t-tests were carried out to evaluate significant differences in surface roughness, cell  
259 counts and copy numbers of Desulfobacteraceae and Desulfobulbaceae among samples. To  
260 compare differences in the microbial communities, one-way unordered Analysis of Similarity  
261 (ANOSIM) was carried out on Primer-E version 7 for both material types and times. Similarity

262 percentage analysis (SIMPER) was also carried out using the Bray-Curtis similarity matrix  
263 generated from the high-throughput sequencing data and Primer-E version 7 to determine which  
264 microbial population contributed most to the differences between material types. All differences  
265 were determined to be significant at the 90% confidence level (i.e.,  $p < 0.10$ ). The confidence  
266 level was set at 90% on the basis that biological samples have a usual baseline variance that may  
267 vary with time, and can contribute to outliers. Hence, setting the confidence level at 90% would  
268 account for differences among treatment but at the same time, do not lower the comparison  
269 power into irrelevance.

270

### 271 **3. Results**

#### 272 **3.1. Surface characteristics of the different materials**

273 Surface roughness and the extent of hydrophobicity were evaluated for the four types of materials.  
274 Polycarbonate exhibited a significantly higher surface roughness than stainless steel ( $p = 0.10$ ) and  
275 titanium ( $p = 0.08$ ). Although the root mean square (RMS) value representative of surface  
276 roughness for HDPE was higher than that for both metals, the values were not significantly higher  
277 (Table 2). All the materials were hydrophilic and had a liquid-surface droplet of contact angle  $<$   
278  $90^\circ$  (Table 2). However, it was observed that both HDPE and polycarbonate were relatively more  
279 hydrophilic than SS316 and titanium.

#### 280 **3.2. Cell counts on different materials**

281 In general, the planktonic cell counts in seawater were lower than the cell counts attached to HDPE,  
282 polycarbonate and titanium but approximately the same as those attached to SS316. To illustrate,  
283 average planktonic cell counts in the seawater during the sampling months were  $9.2 \times 10^5 \pm 7.4 \times$

284  $10^5$  cells/mL and were significantly lower than the cell counts attached to HDPE, polycarbonate  
285 and titanium ( $p < 0.02$ ). However, the average planktonic cell counts in seawater were not  
286 significantly different from those attached to SS316 ( $p = 0.20$ ) (Figure 2). Comparisons of the  
287 attached cell counts among the different materials suggested that 1 month was enough to appreciate  
288 statistically significant differences between SS316 and the rest of materials ( $p < 0.01$ ). The average  
289 cell counts on HDPE, polycarbonate and titanium were  $2.2 \times 10^6 \pm 9.0 \times 10^5$  cells/mL,  $1.9 \times 10^6 \pm$   
290  $7.6 \times 10^5$  cells/mL, and  $7.9 \times 10^5 \pm 1.9 \times 10^4$  cells/mL, respectively. These counts were more than  
291 1-log higher the one attached to SS316 ( $7.2 \times 10^4 \pm 5.0 \times 10^3$ ) cells/mL. At 2<sup>nd</sup> and 4<sup>th</sup> month, the  
292 cell counts on SS316 remained significantly lower than those attached to the other three types of  
293 materials ( $p < 0.01$ , reaching a maximum value of  $2.8 \times 10^5$  cells/mL in the 4 months of operation  
294 (Figure 2). There were no significant differences in the attached cell counts on HDPE,  
295 polycarbonate and titanium throughout the sampling months ( $p > 0.10$ ).

### 296 **3.3. Variations in microbial communities attached to different materials compared to those** 297 **in planktonic seawater**

298 The microbial community was assessed using 16S rRNA gene-based amplicon sequencing. The  
299 relative abundance of each genus and unclassified microbial group was used for multivariate  
300 analysis and represented on a metric multidimensional scaling (mMDS) plot (Figure 3A).

301 Overall, the sample groupings indicate differences in the microbial communities attached to four  
302 types of materials compared to those in planktonic seawater. One-way ANOSIM revealed R  
303 statistic values of 0.171, 0.436, 0.382 and 0.357 between seawater and SS316, titanium, HDPE  
304 or polycarbonate, respectively ( $p < 0.10$ ) (Table 3A).

305 The first difference between seawater and an attached biofilm microbial community was the  
306 number of unique operational taxonomic units (OTUs). To illustrate, at a sequencing depth of

307 2715 sequences, there was an average of 905 OTUs identified for SS316 throughout the study  
308 period, while the other materials had at least 1.2 times higher numbers of OTUs. However, the  
309 numbers of OTUs identified in the biofilms of all four materials were, on average, lower than the  
310 1350 unique OTUs detected in the seawater.

311 The second difference between the microbial communities in seawater and in attached biofilms  
312 was the relative abundance of several microbial taxa. Unclassified Bacteria, unclassified  
313 Alphaproteobacteria and Bacillariophyta were the predominant groups present in a relative  
314 abundance of > 8% on all the materials. Both the unclassified bacteria and the unclassified  
315 Alphaproteobacteria were also present in relative abundances of 29.3% and 11.0% of the total  
316 microbial community, respectively, in the seawater (Figure 4). However, Bacillariophyta was  
317 present in an average relative abundance of only 0.8% in the seawater, and SIMPER analysis  
318 revealed that Bacillariophyta was the taxa (Figure 4) that accounted for an average of 6.3% of  
319 the difference between the microbial community in seawater and the communities attached to the  
320 materials (Supplementary S1). In addition, *Candidatus Pelagibacter* and unclassified  
321 Rhodobacteraceae were more abundant in the seawater than in the biofilms attached to all the  
322 materials (Figure 4), and they contributed to an additional percentage of approximately 3.2% of  
323 the difference between seawater and the attached biofilms.

#### 324 **3.4. Variations in the microbial communities attached to different materials**

325 As observed in Figure 3A, the sample groups showed differences in the microbial communities  
326 attached to the HDPE and polycarbonate compared to those attached to titanium or SS316. The  
327 microbial communities on HDPE and polycarbonate showed a similarity of 65.2%, but they only  
328 shared an average of 53.7% similarity with the microbial communities attached to both types of  
329 metal. One-way ANOSIM analyses revealed significant differences between SS316 compared

330 with HDPE and polycarbonate at the 90% confidence level (Table 3A). To illustrate, the R  
331 statistic of SS316 against HDPE and polycarbonate were 0.163 ( $p = 0.05$ ) and 0.133 ( $p = 0.10$ ),  
332 while the R statistics of titanium against HDPE and polycarbonate were 0.128 ( $p = 0.13$ ) and  
333 0.149 ( $p = 0.11$ ), respectively. There was also no significant difference between the microbial  
334 community attached to SS316 and titanium (One-way ANOSIM,  $p = 0.31$ ).

335 SIMPER analysis revealed that Bacillariophyta and unclassified Planctomycetaceae were the  
336 predominant groups and contributed to a 13% cumulative difference in the microbial communities  
337 on metal and plastic (Supplementary S1). These taxa were present at relative abundances of 14.5%  
338 and 4.0% on the metals, respectively (Figure 4). In contrast, Bacillariophyta accounted for a  
339 relative abundance of 28.6% on the plastic materials while unclassified Planctomycetaceae  
340 accounted for  $< 1\%$  of the total microbial communities attached to the plastics (Figure 4). SIMPER  
341 analysis also showed that titanium supported a higher diversity of different microbial populations,  
342 specifically, GpIV, *Kangiella*, unclassified Enterobacteriaceae, unclassified Cyanobacteria and  
343 *Lutaonella*, which were present in  $> 2\%$  relative abundance on the titanium (Figure 4) and  
344 contributed to approximately 12% of the cumulative difference between the microbial  
345 communities on titanium and plastic materials (Supplementary S1).

### 346 **3.5. Temporal variation of seawater biofilm**

347 Cell counts attached as biofilm on HDPE and polycarbonate remained at the same level of  $\sim 10^6$   
348 cells/mL throughout the sampling months (Figure 2). In contrast, the 3-month-old biofilm  
349 attached to titanium increased by more than 1-log to  $1.7 \times 10^7 \pm 9.3 \times 10^4$  cells/mL compared to  
350 1-month-old biofilm ( $7.9 \times 10^5 \pm 1.9 \times 10^4$  cells/mL). The mature biofilm from SS316 sampled at  
351 the 4<sup>th</sup> month also had approximately 3-fold higher cell counts than the 1-month and 2-month  
352 biofilms from the same material (Figure 2). Multivariate analysis of the relative abundances of



353 the bacterial genera present in the biofilms sampled throughout the four-month period revealed a  
354 temporal succession in the microbial populations (Figure 3B). However, one-way ANOSIM  
355 revealed no significant difference in the overall microbial communities among the 4 sampling  
356 months (Table 3B).

### 357 **3.6. Occurrence of opportunistic pathogen genera on different materials**

358 Genera associated with opportunistic pathogens that were within the detection limits of the high-  
359 throughput sequencing approach included *Acinetobacter*, *Arcobacter*, *Coxiella*, *Legionella* and  
360 *Pseudomonas*. There were no apparent temporal changes in the relative abundance of  
361 *Arcobacter*, *Legionella* and *Pseudomonas*, and all were present in relative abundances of  $\leq$   
362 0.35% of the total microbial community (Figure 5A). This is with the exception of a single  
363 instance of an exceedingly high relative abundance of *Pseudomonas* (35.1% of total microbial  
364 community) in the 2-month-old biofilm attached to SS316 (Figure 5A). *Acinetobacter* and  
365 *Coxiella* were also present at up to ca. 0.36% of the total microbial community on HDPE and  
366 SS316 (Figure 5A). In particular, the relative abundance of *Coxiella* remained higher in the  
367 biofilm attached to SS316 than in those attached to other materials throughout the 4-month  
368 sampling period.

### 369 **3.7. Occurrence of SRB on different materials**

370 Seawater contains a high sulfate content, which can favor the presence of SRB that are thought  
371 to be the main protagonists in biocorrosion. Emphasis was therefore placed on evaluating the  
372 presence of SRB attached to different materials using both high-throughput amplicon sequencing  
373 and qPCR. The main type of SRB detected in this study included unclassified  
374 Desulfobacteraceae, unclassified Desulfobulbaceae and unclassified Desulfovibrionaceae (Figure

375 5B). The qPCR analyses indicated that there was a 10-fold higher copy number of  
376 Desulfobulbaceae detected on SS316 than on the other materials ( $p < 0.05$ ) (Figure 6). The  
377 average copy number of Desulfobulbaceae attached to SS316 was  $2.1 \times 10^{-3}$  copies/cell number  
378 and was similar to that detected in seawater ( $2.2 \times 10^{-3}$  copies/cell number) ( $p = 0.85$ ). In  
379 contrast, there was no significant difference in the abundance of Desulfobulbaceae attached to  
380 HDPE, polycarbonate and titanium ( $p > 0.20$ ). Desulfobacteraceae was also present in ca. 10-  
381 fold higher abundance than Desulfobulbaceae across all samples, but the amounts attached to the  
382 different materials were significantly lower than those present in seawater (Figure 6) ( $p < 0.10$ ).  
383 To illustrate, the copy number of Desulfobacteraceae present in seawater was  $7.4 \times 10^{-1}$   
384 copies/cell number, while that attached to the SS316 coupons was highest at  $9.5 \times 10^{-2}$   
385 copies/cell number, followed by that on titanium ( $6.3 \times 10^{-2}$  copies/cell number), HDPE ( $3.9 \times$   
386  $10^{-2}$  copies/cell number) and polycarbonate ( $2.6 \times 10^{-2}$  copies/cell number). The abundance of  
387 Desulfobacteraceae present on SS316 was significantly higher than that on HDPE and  
388 polycarbonate ( $p < 0.05$ ) but was not significantly different from that on titanium ( $p = 0.44$ ).  
389 Similarly, there were no significant differences in the abundances of Desulfobulbaceae on  
390 titanium compared with HDPE ( $p = 0.51$ ) or polycarbonate ( $p = 0.31$ ).

391

#### 392 **4. Discussion**

393 The findings in this study demonstrated that different materials have varying extents of surface  
394 roughness and hydrophobicity/hydrophilicity. Unlike an earlier study, which showed that there  
395 was more microbial colonization on rougher surfaces [34], our study revealed no apparent  
396 differences in cell numbers attached to polycarbonate, which has the roughest surface (Table 2),

397 compared to HDPE and titanium. Earlier studies also demonstrated that relatively hydrophilic  
398 surfaces were less prone to cell attachment [35-37]. However, both HDPE and polycarbonate,  
399 which are more hydrophilic than titanium and SS316 (Table 2), had higher attached cell numbers  
400 than SS316 (Figure 2). In addition, the bacterial cell numbers attached to the different materials  
401 showed no significant differences as the biofilms matured with time (Figure 2). This observation  
402 is in agreement with that reported earlier [38, 39]. It is likely that as the biofilm matures,  
403 bacterial cells condition the surfaces of different materials through the production of extracellular  
404 polymeric substances and diminish the role of surface properties in cell attachment.

405         It is therefore likely that other factors, including the antibacterial effect associated with  
406 each type of material, would also affect cell attachment, colonization and biofilm development.  
407 To illustrate, in drinking water, plastic materials such as polyethylene were observed to have a  
408 higher number of attached total bacterial and viral-like particles than copper [14]. Copper is a  
409 heavy metal that was previously shown to inhibit the number of *L. pneumophila* cells in a  
410 biofilm matrix [40]. Similarly, stainless steel is an alloy comprising manganese, silicon,  
411 chromium, nickel and molybdenum, all of which are heavy metals that could possibly impede  
412 cell attachment and development. This likely accounts for the lower cell densities obtained on  
413 stainless steel for both the seawater microbial biofilm assessed in this study (Figure 2) and for  
414 the drinking water biofilm in other studies [11, 12]. Although titanium is also a metal, its effect  
415 contrasted with that of stainless steel. Instead, the total attached cell numbers on titanium were of  
416 the same range as those attached to HDPE and polycarbonate (Figure 2). Earlier studies found  
417 that pure titanium was non-mutagenic and non-cytotoxic [41, 42] and that comparable cell  
418 numbers adhered to titanium and HDPE [42].

419           Regardless, the microbial community structures attached to the two metallic materials  
420 were distinct from those on the two plastic materials. In particular, qPCR revealed that there  
421 were higher copy numbers of Desulfobulbaceae and Desulfobacteraceae when normalized  
422 against the total attached cells number on the stainless steel compared to the other materials  
423 (Figure 6). Both Desulfobulbaceae and Desulfobacteraceae are members of SRB, which are  
424 thought to be the main protagonists for microbial-induced biocorrosion. Their presence on the  
425 stainless steel may have accounted for the occurrence of pitting on the SS316 (data not shown)  
426 but not on any of the other materials tested in this study. Numerous types of SRB, including  
427 *Desulfovibrio vulgaris* [43, 44] and *Desulfobulbus propionicus* [45], are capable of obtaining  
428 electrons from stainless or carbon steel by coupling with sulfate reduction to gain maintenance  
429 energy. This redox reaction, in turn, causes microbial-induced biocorrosion.

430           The higher abundance of Desulfobulbaceae and Desulfobacteraceae on stainless steel can  
431 be accounted for by the presence of sulfur contents present in the stainless steel alloy. The  
432 enrichment of SRB on a conductive matrix was also reported earlier in studies examining the  
433 microbial communities on granular activated carbons (GACs) [46, 47]. Similar to stainless steel,  
434 GACs are derived from lignite containing sulfur and are bound by van der Waals forces at the  
435 molecular level to permit free electron flow (i.e., they are good conductors of electricity).  
436 Similarly, the high relative abundance of *Pseudomonas aeruginosa* associated with the stainless  
437 steel can be accounted for by the fact that *P. aeruginosa* produces pyocyanins as electron transfer  
438 mediators [48, 49] and can, in turn, reduce thiosulfate for its metabolic needs on a conductive  
439 matrix such as stainless steel [50, 51]. In contrast, titanium is not a good conductor of electricity,  
440 with a relative conductivity of approximately 3% compared to that of copper [52]. Furthermore,  
441 based on thermodynamics and kinetics, SRB cannot corrode titanium to obtain energy. These

442 factors may have accounted for the lower abundance of SRB on titanium despite it being a  
443 metallic material.

444 In addition to a higher abundance of Desulfobulbaceae and Desulfobacteraceae, there was  
445 also high relative abundance of *Acinetobacter* and *Coxiella* associated with stainless steel. Both  
446 genera contain species associated with opportunistic pathogens, namely *Acinetobacter*  
447 *baumannii* and *Coxiella burnetii*. In an earlier study, bacterial species isolated from drinking  
448 water were evaluated for their hydrophilicity and hydrophobicity, and it was observed that the  
449 majority of the bacterial isolates, including *Acinetobacter*, were hydrophilic [53]. Since all the  
450 materials evaluated in this study are hydrophilic surfaces, it is likely that *Acinetobacter* adheres  
451 very well compared to the other isolates due to the hydrophilicity effect. However, qPCR did not  
452 show *Acinetobacter baumannii* to be present in any of the samples (data not shown).

453 For the genus *Coxiella*, *C. burnetii* is the only member of this genus currently isolated  
454 and characterized. This species is an obligate intracellular parasite that is commonly detected in  
455 seawater by molecular methods [54], which may explain their occurrence in the seawater  
456 biofilm. It has been postulated that being obligate intracellular parasites [55], species within this  
457 genus may be protected from external environmental factors, including the antibacterial effect of  
458 stainless steel, and may successfully establish itself as one of the bacterial populations in the  
459 biofilms on all the tested materials. However, it remains unknown why this genus would attach  
460 preferentially to stainless steel compared to the other materials.

## 461 **5. Conclusions**

462 Although this study did not assess the impact on cell numbers and microbial community  
463 structure of pipe materials in combination with other factors (e.g., the presence of chlorine

464 disinfectant and/or varying shear force), it is one of the few studies providing a comprehensive  
465 evaluation of the differences in seawater microbial biofilms as a result of attachment to a  
466 material substratum. The findings from this study suggest that certain material types, for example  
467 polycarbonate and HDPE, are preferred by bacterial to attach and establish biofilm. This is  
468 evidenced from the higher cell numbers attached to both materials compared to SS316. Despite a  
469 lower number of cells attached on SS316, there was a selective enrichment of sulfate-reducing  
470 Desulfobacteraceae and Desulfobulbaceae on SS316 compared to the other materials. This may  
471 make the stainless steel piping network relatively prone to biocorrosion. The use of stainless  
472 steel as a piping material in most industrial applications involving seawater usage may not be as  
473 ideal compared to titanium.

## 474 **6. Acknowledgements**

475 The research reported in this publication was supported by CRG funding URF/1/2982-01-01  
476 from King Abdullah University of Science and Technology (KAUST) awarded to P.-Y. Hong.

477

478 **7. References**

- 479 [1] J.A. Hargreaves, 2013, Biofloc production systems for  
480 aquaculture, [https://aquaculture.ca.uky.edu/sites/aquaculture.ca.uky.edu/files/srac\\_4503\\_biofloc\\_pro](https://aquaculture.ca.uky.edu/sites/aquaculture.ca.uky.edu/files/srac_4503_biofloc_production_systems_for_aquaculture.pdf)  
481 [duction\\_systems\\_for\\_aquaculture.pdf](https://aquaculture.ca.uky.edu/sites/aquaculture.ca.uky.edu/files/srac_4503_biofloc_production_systems_for_aquaculture.pdf) (Accessed on 23 May 2017)
- 482 [2] A. Sweity, Y. Oren, Z. Ronen, M. Herzberg, The influence of antiscalants on biofouling of RO  
483 membranes in seawater desalination, *Water Res*, 47 (10) (2013) 3389-3398.
- 484 [3] R. Murga, T.S. Forster, E. Brown, J.M. Pruckler, B.S. Fields, R.M. Donlan, Role of biofilms in the  
485 survival of *Legionella pneumophila* in a model potable-water system, *Microbiology*, 147 (Pt 11) (2001)  
486 3121-3126.
- 487 [4] H.Y. Lau, N.J. Ashbolt, The role of biofilms and protozoa in *Legionella* pathogenesis: implications for  
488 drinking water, *J Appl Microbiol*, 107 (2) (2009) 368-378.
- 489 [5] S.E. Coetsier, T.E. Cloete, Biofouling and biocorrosion in industrial water systems, *Crit Rev Microbiol*,  
490 31 (4) (2005) 213-232.
- 491 [6] H.c.A. Videla, *Manual of biocorrosion*, CRC Press, Boca Raton, 1996.
- 492 [7] J. Silhan, C.B. Corfitzen, H.J. Albrechtsen, Effect of temperature and pipe material on biofilm  
493 formation and survival of *Escherichia coli* in used drinking water pipes: a laboratory-based study, *Water*  
494 *Sci Technol*, 54 (3) (2006) 49-56.
- 495 [8] H. Wang, S. Masters, M.A. Edwards, J.O. Falkinham, 3rd, A. Pruden, Effect of disinfectant, water age,  
496 and pipe materials on bacterial and eukaryotic community structure in drinking water biofilm, *Environ*  
497 *Sci Technol*, 48 (3) (2014) 1426-1435.
- 498 [9] I. Douterelo, R.L. Sharpe, J.B. Boxall, Influence of hydraulic regimes on bacterial community structure  
499 and composition in an experimental drinking water distribution system, *Water Res*, 47 (2) (2013) 503-  
500 516.
- 501 [10] J. Yu, D. Kim, T. Lee, Microbial diversity in biofilms on water distribution pipes of different materials,  
502 *Water Sci Technol*, 61 (1) (2010) 163-171.
- 503 [11] P.L. Waines, R. Moate, A.J. Moody, M. Allen, G. Bradley, The effect of material choice on biofilm  
504 formation in a model warm water distribution system, *Biofouling*, 27 (10) (2011) 1161-1174.
- 505 [12] H.J. Jang, Y.J. Choi, J.O. Ka, Effects of diverse water pipe materials on bacterial communities and  
506 water quality in the annular reactor, *J Microbiol Biotechnol*, 21 (2) (2011) 115-123.
- 507 [13] P. Niquette, P. Servais, R. Savoir, Impacts of pipe materials on densities of fixed bacterial biomass in  
508 a drinking water distribution system, *Water Research*, 34 (6) (2000) 1952-1956.
- 509 [14] M.J. Lehtola, I.T. Miettinen, T. Lampola, A. Hirvonen, T. Vartiainen, P.J. Martikainen, Pipeline  
510 materials modify the effectiveness of disinfectants in drinking water distribution systems, *Water*  
511 *Research*, 39 (10) (2005) 1962-1971.
- 512 [15] M.J. Lehtola, K.T. Miettinen, M.M. Keinanen, T.K. Kekki, O. Laine, A. Hirvonen, T. Vartiainen, P.J.  
513 Martikainen, *Microbiology, chemistry and biofilm development in a pilot drinking water distribution*  
514 *system with copper and plastic pipes*, *Water Research*, 38 (17) (2004) 3769-3779.
- 515 [16] H. Tamaki, Y. Sekiguchi, S. Hanada, K. Nakamura, N. Nomura, M. Matsumura, Y. Kamagata,  
516 Comparative analysis of bacterial diversity in freshwater sediment of a shallow eutrophic lake by  
517 molecular and improved cultivation-based techniques, *Appl Environ Microbiol*, 71 (4) (2005) 2162-2169.
- 518 [17] R.I. Amann, W. Ludwig, K.H. Schleifer, Phylogenetic identification and in situ detection of individual  
519 microbial cells without cultivation, *Microbiol Rev*, 59 (1) (1995) 143-169.
- 520 [18] F.M. AlAbbas, C. Williamson, S.M. Bhola, J.R. Spear, D.L. Olson, B. Mishra, A.E. Kakpovbia, Influence  
521 of sulfate reducing bacterial biofilm on corrosion behavior of low-alloy, high-strength steel (API-5L X80),  
522 *Int Biodeter Biodegr*, 78 (2013) 34-42.

523 [19] G. Wegener, V. Krukenberg, D. Riedel, H.E. Tegetmeyer, A. Boetius, Intercellular wiring enables  
524 electron transfer between methanotrophic archaea and bacteria, *Nature*, 526 (7574) (2015) 587-U315.

525 [20] G. Scarascia, T. Wang, P.Y. Hong, Quorum Sensing and the Use of Quorum Quenchers as Natural  
526 Biocides to Inhibit Sulfate-Reducing Bacteria, *Antibiotics (Basel)*, 5 (4) (2016).

527 [21] D. Enning, J. Garrelfs, Corrosion of iron by sulfate-reducing bacteria: new views of an old problem,  
528 *Appl Environ Microbiol*, 80 (4) (2014) 1226-1236.

529 [22] H.C. Flemming, Economical and technical overview, in: E. Heitz, H.C. Flemming, W. Sand (Eds.)  
530 *Microbially influenced corrosion of materials*, Springer-Verlag Berlin Heidelberg, 1996.

531 [23] P. Rodriguez, 1997, Selection of materials for heat  
532 exchangers, [http://www.iaea.org/inis/collection/NCLCollectionStore/ Public/29/000/29000411.pdf](http://www.iaea.org/inis/collection/NCLCollectionStore/Public/29/000/29000411.pdf)  
533 (Accessed on 15 March)

534 [24] H. Cheng, Y. Xie, L.F. Villalobos, L. Song, K.V. Peinemann, S. Nunes, P.Y. Hong, Antibiofilm effect  
535 enhanced by modification of 1,2,3-triazole and palladium nanoparticles on polysulfone membranes, *Sci*  
536 *Rep*, 6 (2016) 24289.

537 [25] R. Förch, H. Schönherr, A.T.A. Jenkins, *Surface Design: Applications in Bioscience and*  
538 *Nanotechnology*, Wiley, 2009.

539 [26] E. Gatza, F. Hammes, E. Prest, Assessing water quality with the BD Accuri™ C6 flow cytometer, in,  
540 *BD Biosciences*, 2013.

541 [27] P.Y. Hong, E. Wheeler, I.K. Cann, R.I. Mackie, Phylogenetic analysis of the fecal microbial community  
542 in herbivorous land and marine iguanas of the Galapagos Islands using 16S rRNA-based pyrosequencing,  
543 *ISME J*, 5 (9) (2011) 1461-1470.

544 [28] R.C. Edgar, B.J. Haas, J.C. Clemente, C. Quince, R. Knight, UCHIME improves sensitivity and speed of  
545 chimera detection, *Bioinformatics*, 27 (16) (2011) 2194-2200.

546 [29] Q. Wang, G.M. Garrity, J.M. Tiedje, J.R. Cole, Naive Bayesian classifier for rapid assignment of rRNA  
547 sequences into the new bacterial taxonomy, *Appl Environ Microbiol*, 73 (16) (2007) 5261-5267.

548 [30] K. Clarke, R. Gorley, PRIMER version 7: user manual/tutorial, PRIMER-E, Plymouth, UK, 296 (2015).

549 [31] J.R. Cole, Q. Wang, J.A. Fish, B. Chai, D.M. McGarrell, Y. Sun, C.T. Brown, A. Porras-Alfaro, C.R.  
550 Kuske, J.M. Tiedje, Ribosomal Database Project: data and tools for high throughput rRNA analysis,  
551 *Nucleic Acids Res*, 42 (Database issue) (2014) D633-642.

552 [32] M. Harb, C.H. Wei, N. Wang, G. Amy, P.Y. Hong, Organic micropollutants in aerobic and anaerobic  
553 membrane bioreactors: Changes in microbial communities and gene expression, *Bioresour Technol*, 218  
554 (2016) 882-891.

555 [33] N. Al-Jassim, M.I. Ansari, M. Harb, P.Y. Hong, Removal of bacterial contaminants and antibiotic  
556 resistance genes by conventional wastewater treatment processes in Saudi Arabia: Is the treated  
557 wastewater safe to reuse for agricultural irrigation?, *Water Research*, 73 (2015) 277-290.

558 [34] W.G. Characklis, G.A. McFeters, K.C. Marshall, Physiological ecology in biofilm systems, in: W.G.  
559 Characklis, K.C. Marshall (Eds.) *Biofilms*, John Wiley & Sons, New York, 1990, pp. 341-394.

560 [35] M. Fletcher, G.I. Loeb, Influence of substratum characteristics on the attachment of a marine  
561 pseudomonad to solid surfaces, *Appl Environ Microbiol*, 37 (1) (1979) 67-72.

562 [36] J.H. Pringle, M. Fletcher, Influence of substratum wettability on attachment of freshwater bacteria  
563 to solid surfaces, *Appl Environ Microbiol*, 45 (3) (1983) 811-817.

564 [37] B. Bendinger, H.H. Rijnaarts, K. Altendorf, A.J. Zehnder, Physicochemical cell surface and adhesive  
565 properties of coryneform bacteria related to the presence and chain length of mycolic acids, *Appl*  
566 *Environ Microbiol*, 59 (11) (1993) 3973-3977.

567 [38] J. Wingender, H.C. Flemming, Contamination potential of drinking water distribution network  
568 biofilms, *Water Sci Technol*, 49 (11-12) (2004) 277-286.

569 [39] C.M. Pang, P. Hong, H. Guo, W.T. Liu, Biofilm formation characteristics of bacterial isolates retrieved  
570 from a reverse osmosis membrane, *Environ Sci Technol*, 39 (19) (2005) 7541-7550.



571 [40] J. Rogers, A.B. Dowsett, P.J. Dennis, J.V. Lee, C.W. Keevil, Influence of Plumbing Materials on Biofilm  
572 Formation and Growth of *Legionella pneumophila* in Potable Water Systems, *Appl Environ Microbiol*, 60  
573 (6) (1994) 1842-1851.

574 [41] X. Hu, K.G. Neoh, J. Zhang, E.-T. Kang, Bacterial and osteoblast behavior on titanium, cobalt-  
575 chromium alloy and stainless steel treated with alkali and heat: A comparative study for potential  
576 orthopedic applications, *Journal of Colloid and Interface Science*, 417 (2014) 410-419.

577 [42] E. Velasco-Ortega, A. Jos, A.M. Camean, J. Pato-Mourelo, J.J. Segura-Egea, In vitro evaluation of  
578 cytotoxicity and genotoxicity of a commercial titanium alloy for dental implantology, *Mutat Res*, 702 (1)  
579 (2010) 17-23.

580 [43] D. Xu, T. Gu, Carbon source starvation triggered more aggressive corrosion against carbon steel by  
581 the *Desulfovibrio vulgaris* biofilm, *Int Biodeter Biodegr*, 91 (2014) 74-81.

582 [44] P. Zhang, D. Xu, Y. Li, K. Yang, T. Gu, Electron mediators accelerate the microbiologically influenced  
583 corrosion of 304 stainless steel by the *Desulfovibrio vulgaris* biofilm, *Bioelectrochemistry*, 101 (2015) 14-  
584 21.

585 [45] B. Anandkumar, R.P. George, S. Maruthamuthu, N. Palaniswamy, R.K. Dayal, Corrosion behavior of  
586 SRB *Desulfovibrio propionicus* isolated from an Indian petroleum refinery on mild steel, *Materials and*  
587 *Corrosion*, 63 (4) (2012) 355-362.

588 [46] N. LaBarge, Y.D. Yilmazel, P.Y. Hong, B.E. Logan, Effect of pre-acclimation of granular activated  
589 carbon on microbial electrolysis cell startup and performance, *Bioelectrochemistry*, 113 (2017) 20-25.

590 [47] N. LaBarge, Y. Ye, K.-Y. Kim, Y.D. Yilmazel, P.E. Saikaly, P.-Y. Hong, B.E. Logan, Impact of acclimation  
591 methods on microbial communities and performance of anaerobic fluidized bed membrane bioreactors,  
592 *Environmental Science: Water Research & Technology*, 2 (6) (2016) 1041-1048.

593 [48] K. Rabaey, N. Boon, M. Hofte, W. Verstraete, Microbial phenazine production enhances electron  
594 transfer in biofuel cells, *Environ Sci Technol*, 39 (9) (2005) 3401-3408.

595 [49] K. Rabaey, N. Boon, S.D. Siciliano, M. Verhaege, W. Verstraete, Biofuel cells select for microbial  
596 consortia that self-mediate electron transfer, *Appl Environ Microbiol*, 70 (9) (2004) 5373-5382.

597 [50] C.K. Stover, X.Q. Pham, A.L. Erwin, S.D. Mizoguchi, P. Warrenner, M.J. Hickey, F.S. Brinkman, W.O.  
598 Hufnagle, D.J. Kowalik, M. Lagrou, R.L. Garber, L. Goltry, E. Tolentino, S. Westbrook-Wadman, Y. Yuan,  
599 L.L. Brody, S.N. Coulter, K.R. Folger, A. Kas, K. Larbig, R. Lim, K. Smith, D. Spencer, G.K. Wong, Z. Wu, I.T.  
600 Paulsen, J. Reizer, M.H. Saier, R.E. Hancock, S. Lory, M.V. Olson, Complete genome sequence of  
601 *Pseudomonas aeruginosa* PAO1, an opportunistic pathogen, *Nature*, 406 (6799) (2000) 959-964.

602 [51] P.Y. Hong, N. Moosa, J. Mink, Dynamics of microbial communities in an integrated ultrafiltration-  
603 reverse osmosis desalination pilot plant located at the Arabian Gulf, *Desalin Water Treat*, 57 (35) (2016)  
604 16310-16323.

605 [52] TotalMateria, 2005, Physical properties of titanium and its  
606 alloys, <http://www.totalmateria.com/Article122.htm> (Accessed on 3 October 2017)

607 [53] L.C. Simoes, M. Simoes, R. Oliveira, M.J. Vieira, Potential of the adhesion of bacteria isolated from  
608 drinking water to materials, *J Basic Microbiol*, 47 (2) (2007) 174-183.

609 [54] P.M. Erwin, M.C. Pineda, N. Webster, X. Turon, S. Lopez-Legentil, Down under the tunic: bacterial  
610 biodiversity hotspots and widespread ammonia-oxidizing archaea in coral reef ascidians, *ISME J*, 8 (3)  
611 (2014) 575-588.

612 [55] R. Seshadri, I.T. Paulsen, J.A. Eisen, T.D. Read, K.E. Nelson, W.C. Nelson, N.L. Ward, H. Tettelin, T.M.  
613 Davidsen, M.J. Beanan, R.T. Deboy, S.C. Daugherty, L.M. Brinkac, R. Madupu, R.J. Dodson, H.M. Khouri,  
614 K.H. Lee, H.A. Carty, D. Scanlan, R.A. Heinzen, H.A. Thompson, J.E. Samuel, C.M. Fraser, J.F. Heidelberg,  
615 Complete genome sequence of the Q-fever pathogen *Coxiella burnetii*, *Proc Natl Acad Sci U S A*, 100 (9)  
616 (2003) 5455-5460.

617 [56] S. Lucker, D. Steger, K.U. Kjeldsen, B.J. MacGregor, M. Wagner, A. Loy, Improved 16S rRNA-targeted  
618 probe set for analysis of sulfate-reducing bacteria by fluorescence in situ hybridization, *J Microbiol*  
619 *Methods*, 69 (3) (2007) 523-528.

620 [57] G. Muyzer, E.C. de Waal, A.G. Uitterlinden, Profiling of complex microbial populations by denaturing  
621 gradient gel electrophoresis analysis of polymerase chain reaction-amplified genes coding for 16S rRNA,  
622 *Appl Environ Microbiol*, 59 (3) (1993) 695-700.

623 [58] A. Loy, A. Lehner, N. Lee, J. Adamczyk, H. Meier, J. Ernst, K.H. Schleifer, M. Wagner, Oligonucleotide  
624 microarray for 16S rRNA gene-based detection of all recognized lineages of sulfate-reducing prokaryotes  
625 in the environment, *Appl Environ Microbiol*, 68 (10) (2002) 5064-5081.

626 [59] M.J. McConnell, A. Perez-Ordóñez, P. Perez-Romero, R. Valencia, J.A. Lepe, I. Vázquez-Barba, J.  
627 Pachon, Quantitative real-time PCR for detection of *Acinetobacter baumannii* colonization in the  
628 hospital environment, *J Clin Microbiol*, 50 (4) (2012) 1412-1414.

629

630

631 **Table 1.** Primers used for quantitative PCR.

<b>Target</b>	<b>Primer name</b>	<b>Sequences (5'-3')</b>	<b>Reference</b>
Desulfobacteraceae (16S rRNA genes)	DSBAC357F	GTGAGGAATTTTGC GCAATGG	[56]
	519R	GWATTACCGCGGCKGCTG	[57]
Desulfobulbaceae (16S rRNA genes)	519F	CAGCMGCCGCGGTAATWC	[57]
	DSB706R	ACCGGTATTCTCCCGAT	[58]
<i>Acinetobacter baumannii</i> ( <i>ompA</i> gene)	<i>ompA</i> -F	TCTTGGTGGTCACTTGAAGC	[59]
	<i>ompA</i> -R	ACTCTTGTGGTTGTGGAGCA	

632

633

634 **Table 2.** Surface characteristics of the tested materials.

	<b>Average root mean square, RMS, of surface (n = 3) ± standard deviation</b>	<b>Average liquid-solid contact angle (n = 6) ± standard deviation</b>
HDPE	0.24 ± 0.18 <sup>a</sup>	63.9° ± 1.8°
Polycarbonate	0.53 ± 0.20 <sup>b</sup>	61.6° ± 1.7°
Titanium	0.19 ± 0.11 <sup>a</sup>	80.2° ± 1.5°
Stainless steel SS316	0.19 ± 0.06 <sup>a</sup>	75.6° ± 0.9°

635 a, b Homogenous subgroups by two-tailed t-test method with a significance level of 0.10

636

637 **Table 3.** ANOSIM R statistic values and p-values between the **(A)** different materials, and **(B)** sampling  
 638 months. Values in bold refer to significant differences between the sample pairs at the 90% confidence  
 639 level.

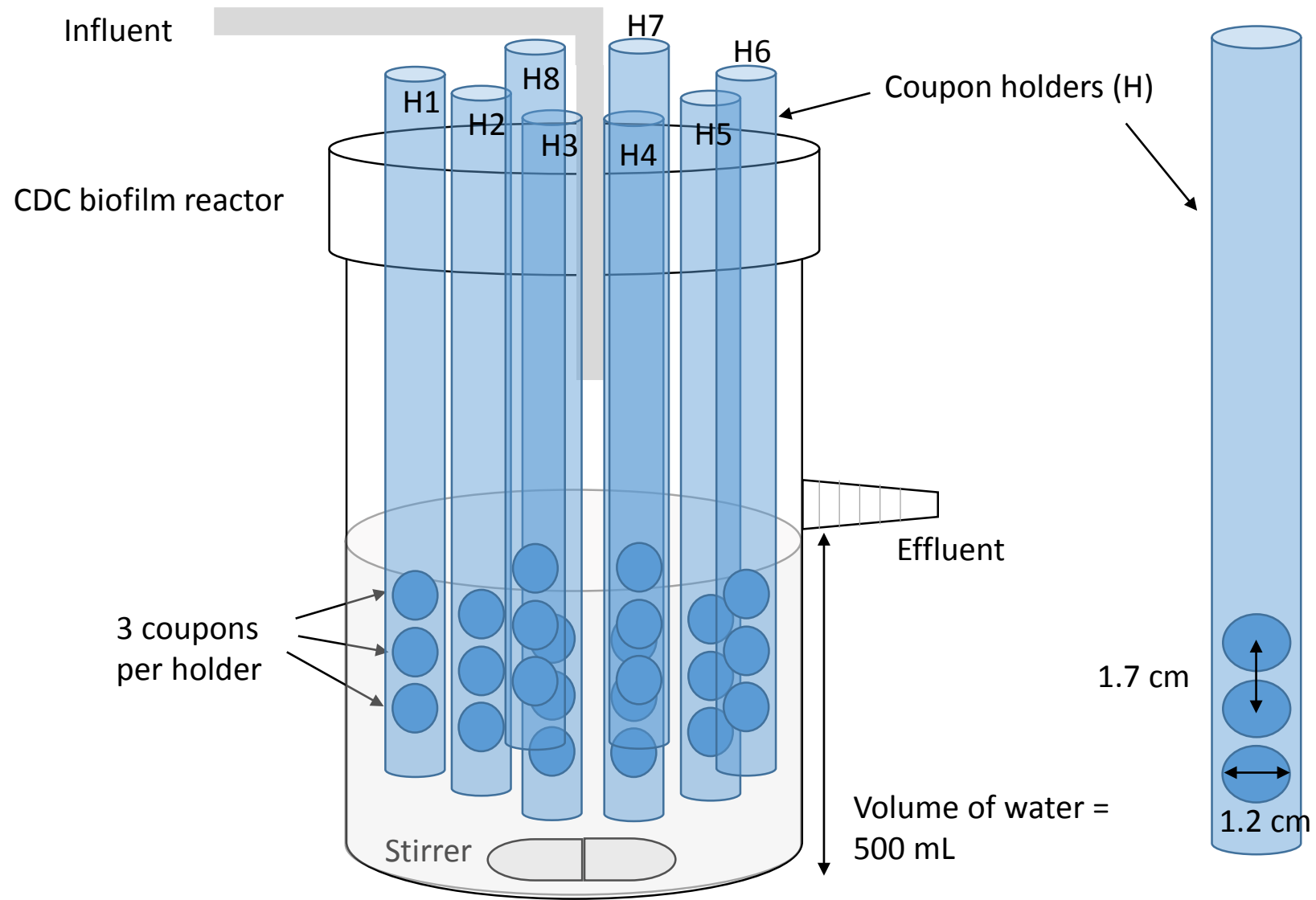
640  
 641

<b>A.</b>	Seawater	HDPE	Polycarbonate	Titanium	SS316
Seawater		<b>0.382</b> (p = <b>0.008</b> )	<b>0.357</b> (p = <b>0.011</b> )	<b>0.436</b> (p = <b>0.016</b> )	<b>0.171</b> (p = <b>0.065</b> )
HDPE			-0.139 (p = 0.967)	-0.128 (p = 0.133)	<b>0.163</b> (p = <b>0.054</b> )
Polycarbonate				0.149 (p = 0.108)	<b>0.133</b> (p = <b>0.100</b> )
Titanium					0.037 (p = 0.305)
SS316					

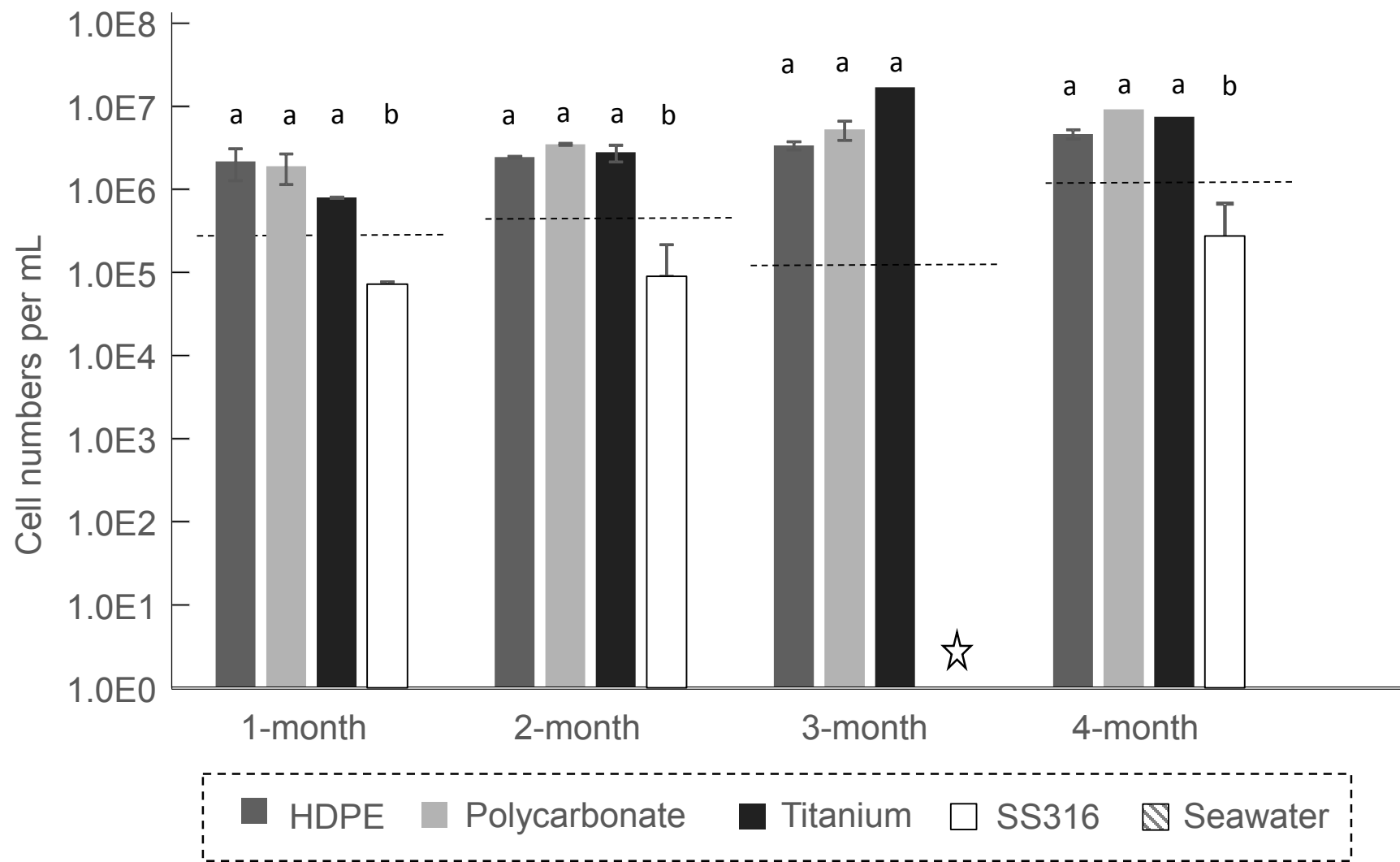
642  
 643

<b>B.</b>	1-month	2-month	3-month	4-month
1-month		0.041 (p = 0.309)	-0.005 (p = 0.485)	0.125 (p = 0.115)
2-month			0.058 (p = 0.228)	0.087 (p = 0.146)
3-month				-0.009 (p = 0.404)
4-month				

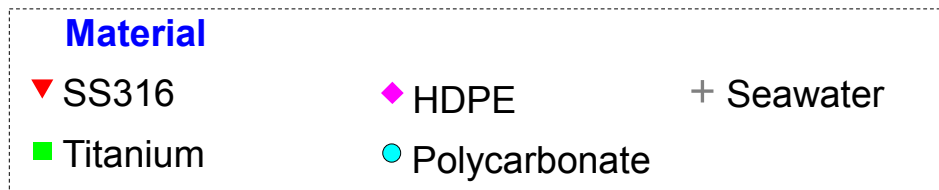
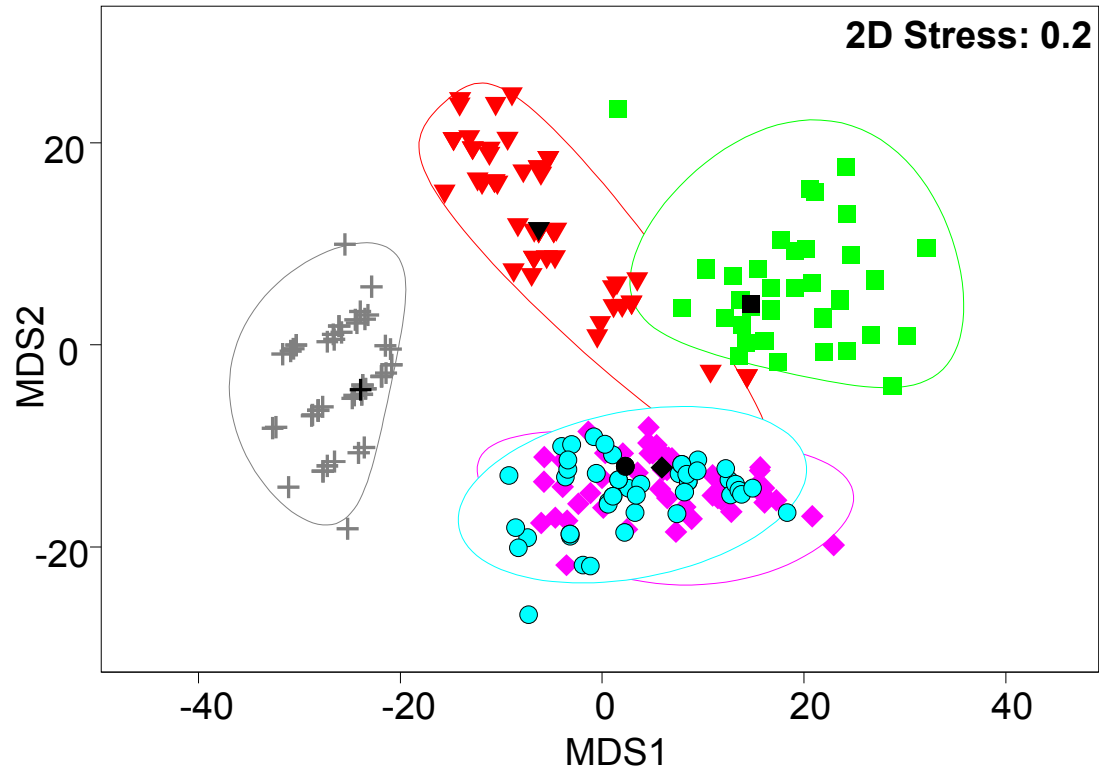
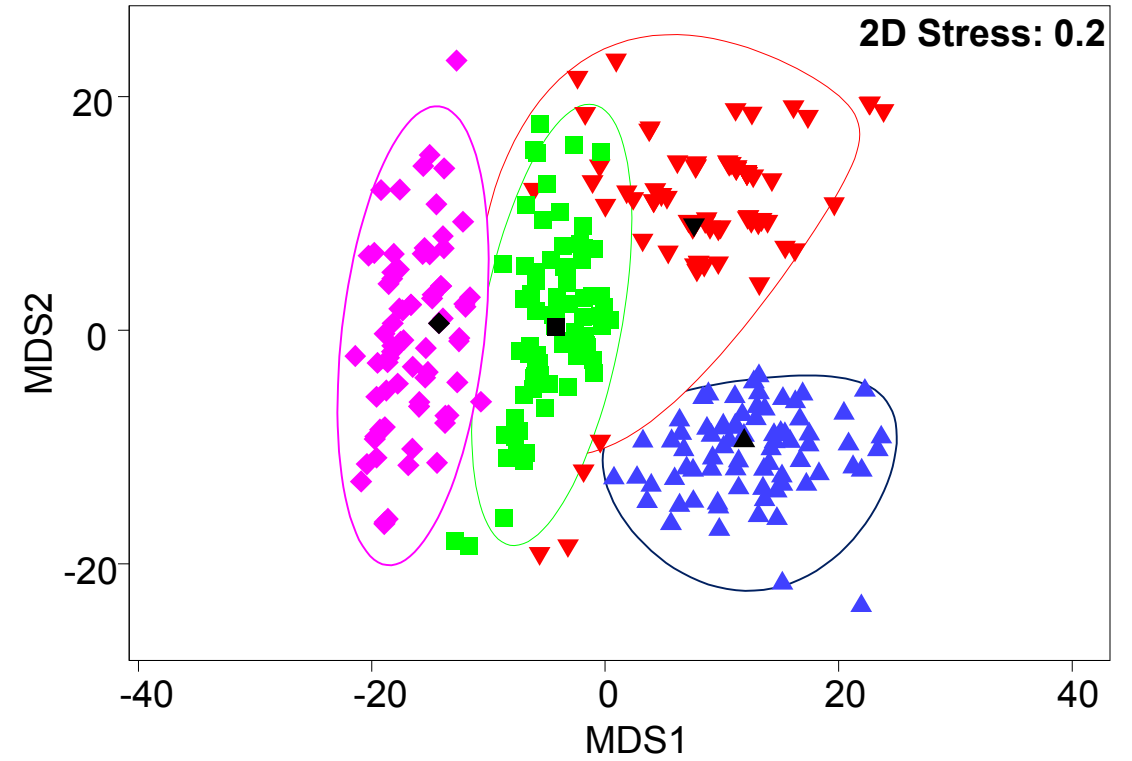
644  
 645  
 646  
 647



**Figure 1.** Illustration of the CDC biofilm reactor.



**Figure 2.** Enumeration of total cell counts attached to different types of materials over a duration of four months. The star denotes no measurements obtained for that sampling month for SS316 due to sampling error. a, b denote homogenous subgroups by two-tailed t-test method with a significance level of 0.10. Dash lines correspond to the cell numbers per mL of seawater at that month. Star denotes no measurements were obtained for that sampling month for stainless steel.

**(A)****(B)**

**Figure 3.** Bootstrapped metric multidimensional scaling (MDS) plots of microbial communities in relation to **(A)** the type of material and **(B)** the temporal effect.



1           **Bacterial cell numbers and community structures of seawater biofilms depend on the**  
2   **attachment substratum**

3                         Scott A. Yap <sup>1</sup>, Giantommaso Scarascia <sup>1</sup>, Pei-Ying Hong <sup>1</sup>

4           <sup>1</sup> King Abdullah University of Science and Technology (KAUST), Water Desalination and Reuse Center  
5   (WDRC), Biological and Environmental Science & Engineering  
6   Division (BESE), Thuwal, 23955-6900, Saudi Arabia

10       **\* Corresponding author:**

11       Pei-Ying Hong

12       Email: [peiying.hong@kaust.edu.sa](mailto:peiying.hong@kaust.edu.sa)

13       Phone: +966-12-8082218

15       **Contact details of co-authors:**

16       Scott A. Yap:

17       Email: [scott.yap@kaust.edu.sa](mailto:scott.yap@kaust.edu.sa)

19       Giantommaso Scarascia:

20       Email: [giantommaso.scarascia@kaust.edu.sa](mailto:giantommaso.scarascia@kaust.edu.sa)

23       **Keywords:** Biofouling, biocorrosion, titanium, stainless steel, polyethylene, polycarbonate, sulfate-  
24       reducing bacteria

25       **Running title:** Seawater biofilm on plastic and metal surfaces

27 **Abstract**

28 Seawater is increasingly being used as a source for various industrial applications. For such  
29 applications, biofilm growth creates various problems including but not limited to pipe  
30 biocorrosion. In this study, it is hypothesized that the material type is preferred by certain  
31 bacterial populations in the seawater to attach and establish biofilms. By comparing differences  
32 in the total cell counts and microbial communities attached to high density polyethylene (HDPE),  
33 polycarbonate, stainless steel (SS316) and titanium, the appropriate material can be used to  
34 minimize biofilm growth. All four materials have hydrophilic surfaces, but polycarbonate  
35 exhibits higher surface roughness. There were no significant differences in the cell numbers  
36 attached to polycarbonate, HDPE and titanium. Instead, there were significantly fewer cells  
37 attached to SS316. However, there was a higher relative abundance of genera associated with  
38 opportunistic pathogens on SS316. Copy numbers of genes representing Desulfobacteraceae and  
39 Desulfobulbaceae, both of which are sulfate-reducing bacteria (SRB), were approximately 10-  
40 fold higher in biofilms sampled from SS316. The enrichment of SRB in the biofilm associated  
41 with SS316 indicates that this material may be prone to biocorrosion. This study highlights the  
42 need for industries to consider the choice of material used in seawater applications to minimize  
43 microbial-associated problems.

44

## 45 **1. Introduction**

46           Seawater is increasingly being used as a source for various industrial applications in an  
47 attempt to alleviate the demand for freshwater. Examples of such industrial applications include  
48 seawater cooling tower systems and seawater injection for enhanced oil recovery. In most  
49 instances, seawater is usually recirculated at least once to minimize operating costs associated  
50 with continuous pumping of new seawater into the system. However, recirculating seawater  
51 allows for microbes, minerals and nutrients to accumulate within the system [1]. To tackle  
52 inorganic scaling problems arising from minerals, antiscalants are commonly used even though  
53 they generally include components of polymers, phosphates and phosphonates and can contribute  
54 nutrients that support microbial growth [2]. Hence, extensive biofilm growth is an inevitable  
55 problem in seawater pipelines.

56           Biofilm growth creates a suite of problems. For example, biofilms can serve as  
57 colonization platforms for pathogens to augment their environmental persistence [3, 4]. Biofilm  
58 formation is also correlated with the occurrence of biocorrosion [5], otherwise known as  
59 microbial-induced corrosion (MIC). This is shown by an increased rate of corrosion in the  
60 presence of biofilms [6]. Although total eradication of biofilms and the associated microbial  
61 populations would be impractical, efforts have been undertaken to minimize cell counts and  
62 bacterial populations that may be present in the biofilm by varying certain operational factors.  
63 These factors include maintaining the presence of residual disinfectant, optimizing water age,  
64 hydraulic regimes and pipe materials [7-15].

65           However, most of the existing studies utilized culture-based approaches or DNA-based  
66 fingerprinting techniques to determine potential impacts on the biofilm arising from these  
67 operational factors. Cultivation-based approaches to enumerating cell counts are subject to bias

68 and are not representative of bacterial species that are fastidious about growth conditions [16,  
69 17]. When compared to high-throughput amplicon-based sequencing approaches, fingerprinting  
70 techniques, including denaturing gel electrophoresis or terminal restriction length  
71 polymorphisms, are not able to provide an in-depth characterization of the bacterial community  
72 structure. Neither are the fingerprinting techniques capable of providing quantitative  
73 measurements of certain bacterial populations when compared to the quantitative PCR (qPCR)  
74 approach. An earlier study used high-throughput sequencing to show that bacterial and/or  
75 eukaryotic community structures in drinking water biofilms can be affected by these factors.  
76 Specifically, pipe materials only affect the bacterial community structure but not the eukaryotic  
77 community [8]. However, similar studies on the variation of cell counts and bacterial community  
78 structures in seawater in relation to the pipe materials are not widely available.

79 A better understanding of whether material types result in differences in microbial  
80 populations, specifically, sulfate-reducing bacteria (SRB) and genera associated with  
81 opportunistic pathogens, is needed to assess the potential relevance to industrial stakeholders and  
82 public health. SRB possess organic filaments similar to nanowires [18], which may play a role in  
83 adhesion, biofilm formation and direct interspecies electron transfer [19]. Adherence to a  
84 conductive material may facilitate extracellular electron transfer and metal reduction, both of  
85 which are key metabolic traits required by the SRB [20]. As such, SRB are generally thought to  
86 be the protagonist in biocorrosion [21]. Biocorrosion is believed to account for 20% of the  
87 damage caused by corrosion [22], which can impart a tremendous financial burden on industrial  
88 stakeholders. In addition, the presence of opportunistic pathogens can also pose potential health  
89 threats to certain groups of individuals, for example, immunocompromised patients, the elderly  
90 and infants, upon exposure.

91           In this study, it is hypothesized that the material type is preferred by certain bacterial  
92 populations in the seawater to attach and establish biofilms. It is further hypothesized that the  
93 type of material plays a less significant role in affecting the total cell count and composition of  
94 the microbial community as the biofilm ages. The materials tested were stainless steel 316 (i.e.,  
95 SS316), titanium, high density polyethylene (HDPE) and polycarbonate. SS316 and titanium are  
96 commonly used in the heat exchangers [23] for industrial seawater applications. HDPE and  
97 polycarbonate are included in this study to serve as non-metal controls and because they are  
98 plastic materials commonly used in industrial applications. Efforts were made to determine the  
99 effect of materials on the genera associated with opportunistic pathogens and sulfate-reducing  
100 bacteria (SRB). To address these issues, counts of cells adhering to the different type of materials  
101 were enumerated by flow cytometry, while both high-throughput sequencing and qPCR were  
102 utilized to characterize the microbial community structures.

103

## 104 **2. Materials and methods**

### 105 **2.1. Experimental procedure**

106 The materials tested in this study were stainless steel 316 (i.e., SS316), titanium, high density  
107 polyethylene (HDPE) and polycarbonate. These materials were characterized for their surface  
108 roughness and hydrophilicity as detailed in Section 2.2. The materials were then placed inside  
109 bioreactors and exposed to seawater over a period of four months (Section 2.3). Seawater biofilm  
110 established on the materials were harvested using sampling procedure described in Section 2.4.  
111 The harvested samples were divided into two portions. The first portion was determined for the  
112 total bacterial cell counts by flow cytometry (Section 2.5). The second portion was extracted for  
113 DNA (Section 2.6), and the DNA was used in two types of molecular-based analyses. The first  
114 molecular-based analysis was 16S rRNA gene amplicon sequencing to characterize the microbial  
115 community attached on the different materials (Section 2.7). The second molecular-based  
116 analysis was quantitative PCR (qPCR) to quantify for the copy numbers of *Acinetobacter*  
117 *baumannii* (Section 2.8), Desulfobacteraceae and Desulfobulbaceae (Section 2.9).

### 118 **2.2. Material surface characterization**

119 The materials tested in this study were purchased from Biosurface Technologies (Bozeman, MT,  
120 USA) in a circular disc coupon format, each with a diameter of approximately 1.2 cm. All the  
121 materials that were tested in this study were evaluated for their surface roughness and extent of  
122 hydrophobicity based on procedures described previously [24]. Briefly, atomic force microscopy  
123 (AFM) was used to characterize the surface topography of each material type based on the  
124 standard protocol defined by American Society of Mechanical Engineer (ASME) B46.1-2009.  
125 AFM imaging was performed using Bruker Dimension ICON equipment (Santa Barbara, CA,  
126 USA) in soft tap mode to scan images of 15  $\mu\text{m}$  width by 15  $\mu\text{m}$  length at three random locations

127 on each material type. The AFM images were analyzed on Pico Image Software (Keysight  
128 Technologies Inc., Santa Rosa, CA, USA). Specifically, surface roughness is represented as the  
129 root mean square (RMS) average of profile height deviations from the mean height observed for  
130 that particular material. A higher RMS value indicates more apparent surface peaks and valleys,  
131 thus representing a rougher surface. The contact angle was measured by an Easy Drop Shape  
132 Analyzer (Kruss, Hamburg, Germany) in static mode at ambient temperature. Ultra-pure water  
133 was used as the probing liquid, and the mean values were determined from three different  
134 independent specimens. Generally, if the contact angle is smaller than  $90^\circ$ , the solid surface is  
135 considered hydrophilic and vice versa [25].

### 136 **2.3. Biofilm reactor operation**

137 From February to June 2016, a total of four Communicable Disease Centre (CDC) bioreactors  
138 (BioSurface Technologies, Bozeman, MT, USA) were operated at  $28^\circ\text{C}$  and at a stirring rate of  
139 200 rpm in the KAUST Water Desalination and Reuse Center (WDRC) (Figure 1). Each  
140 bioreactor had eight coupon holders that could be fitted with a total of 24 coupons of the same  
141 material per reactor. Seawater fed into the bioreactors was sourced from the Red Sea through an  
142 approximately 1 km pipeline to the WDRC laboratory. The seawater tap was flushed for 10  
143 minutes prior to collection of seawater in a sterile 20 L carboy container. Thereafter, seawater  
144 from the same container was fed at a continuous rate of 1.3 mL per minute to each bioreactor and  
145 replaced with fresh seawater every 10 days. The hydraulic retention time of seawater within the  
146 bioreactor was 6.4 h. The bioreactors were periodically checked for the hydraulic retention time,  
147 stirring rate, temperature and flow rate so as to ensure that the operating conditions among all  
148 four reactors are kept similar. Two L of seawater that was to be fed into the reactors were  
149 collected each month during the course of the experiment and evaluated for its total cell counts

150 and microbial community in accordance with protocols mentioned in the following subsections.  
151 All the bioreactors were covered with aluminum foil to limit exposure to light.

#### 152 **2.4. Sampling procedure**

153 Biofilm was sampled at 1 through 4 months after the commencement of the bioreactors. Six  
154 coupons for each type of material were collected during each sampling month and provided two  
155 sets of biological replicates for that particular sampling month. Each biological replicate  
156 comprised the pooled biomass scraped down from three coupons. The six coupons were selected  
157 from two coupon holders placed at random locations within the bioreactor to minimize any  
158 sampling bias due to the location of the coupon. New holders containing coupons of the same  
159 material type were replaced after each sampling event to ensure that the shear force was kept  
160 constant within the bioreactor. The sampled coupons were placed into separate petri dishes, and  
161 5 mL of 1X phosphate-buffered saline (PBS) solution was added. Autoclaved cotton swabs were  
162 then used to scrape down the loosely attached biofilm into the 1X PBS. The resulting suspension  
163 for each material was transferred to sterile 50 mL centrifuge tubes. The used cotton swabs and  
164 coupons were placed in a sterile centrifuge tube that contained 10 mL of 1X PBS. This tube was  
165 vortexed at high speed for 10 minutes with the aim of dislodging any attached biofilm on the  
166 cotton swab and coupons. Following this, the supernatant from each vortexed tube was  
167 transferred to the corresponding tube containing the loosely attached biofilm. A 20  $\mu$ L sample of  
168 the combined supernatant was set aside for total cell enumeration by flow cytometry. The  
169 remaining supernatant was centrifuged at 8000 g for 10 minutes, and the cell pellet was used for  
170 DNA extraction.

#### 171 **2.5. Flow cytometry to obtain total cell counts**



172 A 7  $\mu$ L sample of the supernatant or seawater was diluted 100-fold with 1X PBS, and 10  $\mu$ L of  
173 500 mM ethylenediaminetetraacetic acid (EDTA) was added to chelate metals and other  
174 inhibitors that can affect flow cytometry measurements. The mixture was briefly vortexed and  
175 incubated at 35 °C for 20 minutes. Then, 7  $\mu$ L of 100X SYBR Green I (Thermo Fisher Scientific,  
176 Carlsbad, CA, USA) was added, and the samples were incubated for 10 minutes. The number of  
177 cells in the resultant mixture was then quantified using a BD Accuri C6 (Thermo Fisher  
178 Scientific, Carlsbad, CA, USA) flow cytometer, based on protocol described by manufacturer  
179 [26].

## 180 **2.6. DNA extraction**

181 The microbial DNA from the biofilms was extracted using the UltraClean® PowerSoil DNA  
182 Isolation kit following the manufacturer's protocol with brief modifications as described  
183 previously [27]. To extract DNA from seawater, 2 L of seawater was first filtered through a 0.22  
184  $\mu$ m polycarbonate membrane filter (VWR, Radnor, PA, USA), and the retained biomass on the  
185 filter was extracted using a protocol similar to the one mentioned previously. The DNA  
186 concentration was then quantified using the Qubit Broad Range DNA Assay according to the  
187 manufacturer's protocol. The DNA was used for molecular-based analyses detailed in Section  
188 2.7 to 2.9.

## 189 **2.7. 16S rRNA gene-based amplicon sequencing and amplicon sequencing data analysis**

190 16S rRNA genes were amplified from the DNA with primer pair 515F and 907R based on  
191 procedures described earlier [24]. Purified amplicons were pooled and submitted to the KAUST  
192 Genomics Core lab for sequencing on the Illumina MiSeq platform. All high-throughput  
193 sequencing data were deposited in European Nucleotide Archive under accession number

194 PRJEB20120. The two main hypotheses of this study are that first, certain bacterial populations  
195 in the seawater prefer to attach to specific types of material prior to biofilm formation, and  
196 second, the type of material plays a less significant role in affecting the total cell count and  
197 composition of the microbial community as the biofilm ages. Amplicon sequences that denote  
198 the microbial community were therefore analyzed to test these two hypotheses. Sequences were  
199 sorted by the Bioinformatics Team at KAUST based on a Phred score of  $> 20$ . The sorted  
200 sequences were then trimmed off for the primers, barcodes and adaptor sequences, and any  
201 sequences  $> 300$  nt in length were removed. Chimeras were identified and removed on UCHIME  
202 [28] by comparison with a core reference FASTA file downloaded from Greengenes  
203 (<http://greengenes.lbl.gov/Download/>). Chimera-free sequences were assigned to  
204 bacterial/archaeal taxonomic hierarchy at the 95% classification reliability level using the  
205 Ribosomal Database Project (RDP) Classifier [29]. The relative abundances of the bacterial and  
206 archaeal genera were calculated, collated and then square-root transformed. Square-root  
207 transformation was performed to down-weight the dominant taxa and to achieve a better balance  
208 of the abundant and rare species that are present in the samples. This allows the rare species,  
209 which are common in the data generated from high-throughput sequencing, to exert some  
210 influence on the calculation of similarity. The transformed data sets were then computed for their  
211 Bray–Curtis similarities and represented graphically for relative differences in bacterial  
212 community composition among samples aligned against either the materials or the duration of  
213 operation as factors in a boot-strapped metric multidimensional scaling (mMDS) plot. That is,  
214 samples that were further apart from each other shared less similarity than those that were closer  
215 together. All mMDS plots were obtained using Primer-E version 7 [30]. Chimera-free sequences  
216 were also submitted to the RDP pipeline for clustering analysis to identify the number of unique

217 operational taxonomic units (OTUs) with < 97% sequence similarity at each respective  
218 sequencing depth [31]. The number of unique OTUs identified at a sequencing depth of 2715  
219 sequences were collated and used to compare the level of microbial richness among the  
220 individual samples. This sequencing depth was used because this was the lowest number of reads  
221 obtained for one particular sample, and the comparison of the microbial richness across samples,  
222 therefore, had to be standardized at this depth.

## 223 **2.8. Quantitative PCR for *Acinetobacter baumannii***

224 *Acinetobacter baumannii* was chosen as the pathogenic bacterial species in the genus  
225 *Acinetobacter*, and its abundance was determined because this genus was detected in some of the  
226 biofilm samples. Copy numbers of the *ompA* gene representing *Acinetobacter baumannii* were  
227 determined using qPCR with a 7900 HT Applied Biosystems real-time PCR thermal cycler  
228 (Thermo Fisher Scientific, Carlsbad, CA, USA). Sequences of the primer pairs are listed in Table  
229 1. The qPCR standards were prepared as described previously [32, 33]. To produce qPCR  
230 standard curves, plasmid DNAs were diluted in series to form concentrations ranging from  $10^2$  to  
231  $10^8$  copies/ $\mu\text{L}$ . Each reaction volume of 20  $\mu\text{L}$  contained 10  $\mu\text{L}$  of Fast SYBR Green master mix,  
232 0.4  $\mu\text{L}$  of each primer (10  $\mu\text{M}$ ), 1  $\mu\text{L}$  of DNA template and 8.2  $\mu\text{L}$   $\text{H}_2\text{O}$ . The reaction for  
233 amplification was run using an annealing temperature of 60 °C, and the melting curve analysis  
234 was performed with a dissociation cycle which included an increment of temperature from 60 °C  
235 to 95 °C with intervals of 0.5 °C for 5 s each. The threshold cycle ( $C_q$ ) values for each dilution  
236 were plotted against the log-transformed concentration of each dilution. The amplification factor  
237 of the standards was 2.99, and the R-squared value was > 0.98. Amplifications to obtain standard  
238 curves were performed in triplicate, while test amplifications and negative non-template controls  
239 (NTCs) were run in duplicate. All NTCs had no determinable  $C_q$  values. The copy numbers

240 obtained from qPCR reactions were normalized against the total cell numbers obtained by flow  
241 cytometry for the corresponding sample.

## 242 **2.9. Quantitative PCR for SRB**

243 Both the Desulfobacteraceae and Desulfobulbaceae are families comprised of genera associated  
244 with SRB. The copy numbers of 16S rRNA genes representing total Desulfobacteraceae and  
245 Desulfobulbaceae were, therefore, determined to discern the presence and abundance of certain  
246 types of SRB. The qPCR standards for Desulfobacteraceae and Desulfobulbaceae were prepared  
247 by first amplifying the gene fragment with the appropriate primer pairs using DNA extracted  
248 from *Desulfobacter hydrogenophilus* DSM3380 and *Desulfobulbus elongatus* DSM2908 as  
249 bacterial templates. The amplified products were cloned into vectors, and the inserted genes were  
250 sequenced to verify that the sequences were perfectly complementary to the primer target region.  
251 The qPCR reactions were carried out as described above. The amplification factor of the  
252 standards ranged from 1.98 to 2.13 with R-squared values > 0.99. Amplifications to obtain  
253 standard curves were performed in triplicate, while test amplifications and NTCs were run in  
254 duplicate. All NTCs had no determinable C<sub>q</sub> values. Copy numbers obtained from qPCR were  
255 normalized against the total cell numbers obtained by flow cytometry for the corresponding  
256 sample.

## 257 **2.10. Statistical analyses**

258 Two-tailed t-tests were carried out to evaluate significant differences in surface roughness, cell  
259 counts and copy numbers of Desulfobacteraceae and Desulfobulbaceae among samples. To  
260 compare differences in the microbial communities, one-way unordered Analysis of Similarity  
261 (ANOSIM) was carried out on Primer-E version 7 for both material types and times. Similarity

262 percentage analysis (SIMPER) was also carried out using the Bray-Curtis similarity matrix  
263 generated from the high-throughput sequencing data and Primer-E version 7 to determine which  
264 microbial population contributed most to the differences between material types. All differences  
265 were determined to be significant at the 90% confidence level (i.e.,  $p < 0.10$ ). The confidence  
266 level was set at 90% on the basis that biological samples have a usual baseline variance that may  
267 vary with time, and can contribute to outliers. Hence, setting the confidence level at 90% would  
268 account for differences among treatment but at the same time, do not lower the comparison  
269 power into irrelevance.

270

### 271 **3. Results**

#### 272 **3.1. Surface characteristics of the different materials**

273 Surface roughness and the extent of hydrophobicity were evaluated for the four types of materials.  
274 Polycarbonate exhibited a significantly higher surface roughness than stainless steel ( $p = 0.10$ ) and  
275 titanium ( $p = 0.08$ ). Although the root mean square (RMS) value representative of surface  
276 roughness for HDPE was higher than that for both metals, the values were not significantly higher  
277 (Table 2). All the materials were hydrophilic and had a liquid-surface droplet of contact angle  $<$   
278  $90^\circ$  (Table 2). However, it was observed that both HDPE and polycarbonate were relatively more  
279 hydrophilic than SS316 and titanium.

#### 280 **3.2. Cell counts on different materials**

281 In general, the planktonic cell counts in seawater were lower than the cell counts attached to HDPE,  
282 polycarbonate and titanium but approximately the same as those attached to SS316. To illustrate,  
283 average planktonic cell counts in the seawater during the sampling months were  $9.2 \times 10^5 \pm 7.4 \times$

284  $10^5$  cells/mL and were significantly lower than the cell counts attached to HDPE, polycarbonate  
285 and titanium ( $p < 0.02$ ). However, the average planktonic cell counts in seawater were not  
286 significantly different from those attached to SS316 ( $p = 0.20$ ) (Figure 2). Comparisons of the  
287 attached cell counts among the different materials suggested that 1 month was enough to appreciate  
288 statistically significant differences between SS316 and the rest of materials ( $p < 0.01$ ). The average  
289 cell counts on HDPE, polycarbonate and titanium were  $2.2 \times 10^6 \pm 9.0 \times 10^5$  cells/mL,  $1.9 \times 10^6 \pm$   
290  $7.6 \times 10^5$  cells/mL, and  $7.9 \times 10^5 \pm 1.9 \times 10^4$  cells/mL, respectively. These counts were more than  
291 1-log higher the one attached to SS316 ( $7.2 \times 10^4 \pm 5.0 \times 10^3$ ) cells/mL. At 2<sup>nd</sup> and 4<sup>th</sup> month, the  
292 cell counts on SS316 remained significantly lower than those attached to the other three types of  
293 materials ( $p < 0.01$ , reaching a maximum value of  $2.8 \times 10^5$  cells/mL in the 4 months of operation  
294 (Figure 2). There were no significant differences in the attached cell counts on HDPE,  
295 polycarbonate and titanium throughout the sampling months ( $p > 0.10$ ).

### 296 **3.3. Variations in microbial communities attached to different materials compared to those** 297 **in planktonic seawater**

298 The microbial community was assessed using 16S rRNA gene-based amplicon sequencing. The  
299 relative abundance of each genus and unclassified microbial group was used for multivariate  
300 analysis and represented on a metric multidimensional scaling (mMDS) plot (Figure 3A).

301 Overall, the sample groupings indicate differences in the microbial communities attached to four  
302 types of materials compared to those in planktonic seawater. One-way ANOSIM revealed R  
303 statistic values of 0.171, 0.436, 0.382 and 0.357 between seawater and SS316, titanium, HDPE  
304 or polycarbonate, respectively ( $p < 0.10$ ) (Table 3A).

305 The first difference between seawater and an attached biofilm microbial community was the  
306 number of unique operational taxonomic units (OTUs). To illustrate, at a sequencing depth of

307 2715 sequences, there was an average of 905 OTUs identified for SS316 throughout the study  
308 period, while the other materials had at least 1.2 times higher numbers of OTUs. However, the  
309 numbers of OTUs identified in the biofilms of all four materials were, on average, lower than the  
310 1350 unique OTUs detected in the seawater.

311 The second difference between the microbial communities in seawater and in attached biofilms  
312 was the relative abundance of several microbial taxa. Unclassified Bacteria, unclassified  
313 Alphaproteobacteria and Bacillariophyta were the predominant groups present in a relative  
314 abundance of > 8% on all the materials. Both the unclassified bacteria and the unclassified  
315 Alphaproteobacteria were also present in relative abundances of 29.3% and 11.0% of the total  
316 microbial community, respectively, in the seawater (Figure 4). However, Bacillariophyta was  
317 present in an average relative abundance of only 0.8% in the seawater, and SIMPER analysis  
318 revealed that Bacillariophyta was the taxa (Figure 4) that accounted for an average of 6.3% of  
319 the difference between the microbial community in seawater and the communities attached to the  
320 materials (Supplementary S1). In addition, *Candidatus Pelagibacter* and unclassified  
321 Rhodobacteraceae were more abundant in the seawater than in the biofilms attached to all the  
322 materials (Figure 4), and they contributed to an additional percentage of approximately 3.2% of  
323 the difference between seawater and the attached biofilms.

#### 324 **3.4. Variations in the microbial communities attached to different materials**

325 As observed in Figure 3A, the sample groups showed differences in the microbial communities  
326 attached to the HDPE and polycarbonate compared to those attached to titanium or SS316. The  
327 microbial communities on HDPE and polycarbonate showed a similarity of 65.2%, but they only  
328 shared an average of 53.7% similarity with the microbial communities attached to both types of  
329 metal. One-way ANOSIM analyses revealed significant differences between SS316 compared

330 with HDPE and polycarbonate at the 90% confidence level (Table 3A). To illustrate, the R  
331 statistic of SS316 against HDPE and polycarbonate were 0.163 ( $p = 0.05$ ) and 0.133 ( $p = 0.10$ ),  
332 while the R statistics of titanium against HDPE and polycarbonate were 0.128 ( $p = 0.13$ ) and  
333 0.149 ( $p = 0.11$ ), respectively. There was also no significant difference between the microbial  
334 community attached to SS316 and titanium (One-way ANOSIM,  $p = 0.31$ ).

335 SIMPER analysis revealed that Bacillariophyta and unclassified Planctomycetaceae were the  
336 predominant groups and contributed to a 13% cumulative difference in the microbial communities  
337 on metal and plastic (Supplementary S1). These taxa were present at relative abundances of 14.5%  
338 and 4.0% on the metals, respectively (Figure 4). In contrast, Bacillariophyta accounted for a  
339 relative abundance of 28.6% on the plastic materials while unclassified Planctomycetaceae  
340 accounted for  $< 1\%$  of the total microbial communities attached to the plastics (Figure 4). SIMPER  
341 analysis also showed that titanium supported a higher diversity of different microbial populations,  
342 specifically, GpIV, *Kangiella*, unclassified Enterobacteriaceae, unclassified Cyanobacteria and  
343 *Lutaonella*, which were present in  $> 2\%$  relative abundance on the titanium (Figure 4) and  
344 contributed to approximately 12% of the cumulative difference between the microbial  
345 communities on titanium and plastic materials (Supplementary S1).

### 346 **3.5. Temporal variation of seawater biofilm**

347 Cell counts attached as biofilm on HDPE and polycarbonate remained at the same level of  $\sim 10^6$   
348 cells/mL throughout the sampling months (Figure 2). In contrast, the 3-month-old biofilm  
349 attached to titanium increased by more than 1-log to  $1.7 \times 10^7 \pm 9.3 \times 10^4$  cells/mL compared to  
350 1-month-old biofilm ( $7.9 \times 10^5 \pm 1.9 \times 10^4$  cells/mL). The mature biofilm from SS316 sampled at  
351 the 4<sup>th</sup> month also had approximately 3-fold higher cell counts than the 1-month and 2-month  
352 biofilms from the same material (Figure 2). Multivariate analysis of the relative abundances of



353 the bacterial genera present in the biofilms sampled throughout the four-month period revealed a  
354 temporal succession in the microbial populations (Figure 3B). However, one-way ANOSIM  
355 revealed no significant difference in the overall microbial communities among the 4 sampling  
356 months (Table 3B).

### 357 **3.6. Occurrence of opportunistic pathogen genera on different materials**

358 Genera associated with opportunistic pathogens that were within the detection limits of the high-  
359 throughput sequencing approach included *Acinetobacter*, *Arcobacter*, *Coxiella*, *Legionella* and  
360 *Pseudomonas*. There were no apparent temporal changes in the relative abundance of  
361 *Arcobacter*, *Legionella* and *Pseudomonas*, and all were present in relative abundances of  $\leq$   
362 0.35% of the total microbial community (Figure 5A). This is with the exception of a single  
363 instance of an exceedingly high relative abundance of *Pseudomonas* (35.1% of total microbial  
364 community) in the 2-month-old biofilm attached to SS316 (Figure 5A). *Acinetobacter* and  
365 *Coxiella* were also present at up to ca. 0.36% of the total microbial community on HDPE and  
366 SS316 (Figure 5A). In particular, the relative abundance of *Coxiella* remained higher in the  
367 biofilm attached to SS316 than in those attached to other materials throughout the 4-month  
368 sampling period.

### 369 **3.7. Occurrence of SRB on different materials**

370 Seawater contains a high sulfate content, which can favor the presence of SRB that are thought  
371 to be the main protagonists in biocorrosion. Emphasis was therefore placed on evaluating the  
372 presence of SRB attached to different materials using both high-throughput amplicon sequencing  
373 and qPCR. The main type of SRB detected in this study included unclassified  
374 Desulfobacteraceae, unclassified Desulfobulbaceae and unclassified Desulfovibrionaceae (Figure

375 5B). The qPCR analyses indicated that there was a 10-fold higher copy number of  
376 Desulfobulbaceae detected on SS316 than on the other materials ( $p < 0.05$ ) (Figure 6). The  
377 average copy number of Desulfobulbaceae attached to SS316 was  $2.1 \times 10^{-3}$  copies/cell number  
378 and was similar to that detected in seawater ( $2.2 \times 10^{-3}$  copies/cell number) ( $p = 0.85$ ). In  
379 contrast, there was no significant difference in the abundance of Desulfobulbaceae attached to  
380 HDPE, polycarbonate and titanium ( $p > 0.20$ ). Desulfobacteraceae was also present in ca. 10-  
381 fold higher abundance than Desulfobulbaceae across all samples, but the amounts attached to the  
382 different materials were significantly lower than those present in seawater (Figure 6) ( $p < 0.10$ ).  
383 To illustrate, the copy number of Desulfobacteraceae present in seawater was  $7.4 \times 10^{-1}$   
384 copies/cell number, while that attached to the SS316 coupons was highest at  $9.5 \times 10^{-2}$   
385 copies/cell number, followed by that on titanium ( $6.3 \times 10^{-2}$  copies/cell number), HDPE ( $3.9 \times$   
386  $10^{-2}$  copies/cell number) and polycarbonate ( $2.6 \times 10^{-2}$  copies/cell number). The abundance of  
387 Desulfobacteraceae present on SS316 was significantly higher than that on HDPE and  
388 polycarbonate ( $p < 0.05$ ) but was not significantly different from that on titanium ( $p = 0.44$ ).  
389 Similarly, there were no significant differences in the abundances of Desulfobulbaceae on  
390 titanium compared with HDPE ( $p = 0.51$ ) or polycarbonate ( $p = 0.31$ ).

391

#### 392 **4. Discussion**

393 The findings in this study demonstrated that different materials have varying extents of surface  
394 roughness and hydrophobicity/hydrophilicity. Unlike an earlier study, which showed that there  
395 was more microbial colonization on rougher surfaces [34], our study revealed no apparent  
396 differences in cell numbers attached to polycarbonate, which has the roughest surface (Table 2),

397 compared to HDPE and titanium. Earlier studies also demonstrated that relatively hydrophilic  
398 surfaces were less prone to cell attachment [35-37]. However, both HDPE and polycarbonate,  
399 which are more hydrophilic than titanium and SS316 (Table 2), had higher attached cell numbers  
400 than SS316 (Figure 2). In addition, the bacterial cell numbers attached to the different materials  
401 showed no significant differences as the biofilms matured with time (Figure 2). This observation  
402 is in agreement with that reported earlier [38, 39]. It is likely that as the biofilm matures,  
403 bacterial cells condition the surfaces of different materials through the production of extracellular  
404 polymeric substances and diminish the role of surface properties in cell attachment.

405         It is therefore likely that other factors, including the antibacterial effect associated with  
406 each type of material, would also affect cell attachment, colonization and biofilm development.  
407 To illustrate, in drinking water, plastic materials such as polyethylene were observed to have a  
408 higher number of attached total bacterial and viral-like particles than copper [14]. Copper is a  
409 heavy metal that was previously shown to inhibit the number of *L. pneumophila* cells in a  
410 biofilm matrix [40]. Similarly, stainless steel is an alloy comprising manganese, silicon,  
411 chromium, nickel and molybdenum, all of which are heavy metals that could possibly impede  
412 cell attachment and development. This likely accounts for the lower cell densities obtained on  
413 stainless steel for both the seawater microbial biofilm assessed in this study (Figure 2) and for  
414 the drinking water biofilm in other studies [11, 12]. Although titanium is also a metal, its effect  
415 contrasted with that of stainless steel. Instead, the total attached cell numbers on titanium were of  
416 the same range as those attached to HDPE and polycarbonate (Figure 2). Earlier studies found  
417 that pure titanium was non-mutagenic and non-cytotoxic [41, 42] and that comparable cell  
418 numbers adhered to titanium and HDPE [42].

419           Regardless, the microbial community structures attached to the two metallic materials  
420 were distinct from those on the two plastic materials. In particular, qPCR revealed that there  
421 were higher copy numbers of Desulfobulbaceae and Desulfobacteraceae when normalized  
422 against the total attached cells number on the stainless steel compared to the other materials  
423 (Figure 6). Both Desulfobulbaceae and Desulfobacteraceae are members of SRB, which are  
424 thought to be the main protagonists for microbial-induced biocorrosion. Their presence on the  
425 stainless steel may have accounted for the occurrence of pitting on the SS316 (data not shown)  
426 but not on any of the other materials tested in this study. Numerous types of SRB, including  
427 *Desulfovibrio vulgaris* [43, 44] and *Desulfobulbus propionicus* [45], are capable of obtaining  
428 electrons from stainless or carbon steel by coupling with sulfate reduction to gain maintenance  
429 energy. This redox reaction, in turn, causes microbial-induced biocorrosion.

430           The higher abundance of Desulfobulbaceae and Desulfobacteraceae on stainless steel can  
431 be accounted for by the presence of sulfur contents present in the stainless steel alloy. The  
432 enrichment of SRB on a conductive matrix was also reported earlier in studies examining the  
433 microbial communities on granular activated carbons (GACs) [46, 47]. Similar to stainless steel,  
434 GACs are derived from lignite containing sulfur and are bound by van der Waals forces at the  
435 molecular level to permit free electron flow (i.e., they are good conductors of electricity).  
436 Similarly, the high relative abundance of *Pseudomonas aeruginosa* associated with the stainless  
437 steel can be accounted for by the fact that *P. aeruginosa* produces pyocyanins as electron transfer  
438 mediators [48, 49] and can, in turn, reduce thiosulfate for its metabolic needs on a conductive  
439 matrix such as stainless steel [50, 51]. In contrast, titanium is not a good conductor of electricity,  
440 with a relative conductivity of approximately 3% compared to that of copper [52]. Furthermore,  
441 based on thermodynamics and kinetics, SRB cannot corrode titanium to obtain energy. These

442 factors may have accounted for the lower abundance of SRB on titanium despite it being a  
443 metallic material.

444 In addition to a higher abundance of Desulfobulbaceae and Desulfobacteraceae, there was  
445 also high relative abundance of *Acinetobacter* and *Coxiella* associated with stainless steel. Both  
446 genera contain species associated with opportunistic pathogens, namely *Acinetobacter*  
447 *baumannii* and *Coxiella burnetii*. In an earlier study, bacterial species isolated from drinking  
448 water were evaluated for their hydrophilicity and hydrophobicity, and it was observed that the  
449 majority of the bacterial isolates, including *Acinetobacter*, were hydrophilic [53]. Since all the  
450 materials evaluated in this study are hydrophilic surfaces, it is likely that *Acinetobacter* adheres  
451 very well compared to the other isolates due to the hydrophilicity effect. However, qPCR did not  
452 show *Acinetobacter baumannii* to be present in any of the samples (data not shown).

453 For the genus *Coxiella*, *C. burnetii* is the only member of this genus currently isolated  
454 and characterized. This species is an obligate intracellular parasite that is commonly detected in  
455 seawater by molecular methods [54], which may explain their occurrence in the seawater  
456 biofilm. It has been postulated that being obligate intracellular parasites [55], species within this  
457 genus may be protected from external environmental factors, including the antibacterial effect of  
458 stainless steel, and may successfully establish itself as one of the bacterial populations in the  
459 biofilms on all the tested materials. However, it remains unknown why this genus would attach  
460 preferentially to stainless steel compared to the other materials.

## 461 **5. Conclusions**

462 Although this study did not assess the impact on cell numbers and microbial community  
463 structure of pipe materials in combination with other factors (e.g., the presence of chlorine

464 disinfectant and/or varying shear force), it is one of the few studies providing a comprehensive  
465 evaluation of the differences in seawater microbial biofilms as a result of attachment to a  
466 material substratum. The findings from this study suggest that certain material types, for example  
467 polycarbonate and HDPE, are preferred by bacterial to attach and establish biofilm. This is  
468 evidenced from the higher cell numbers attached to both materials compared to SS316. Despite a  
469 lower number of cells attached on SS316, there was a selective enrichment of sulfate-reducing  
470 Desulfobacteraceae and Desulfobulbaceae on SS316 compared to the other materials. This may  
471 make the stainless steel piping network relatively prone to biocorrosion. The use of stainless  
472 steel as a piping material in most industrial applications involving seawater usage may not be as  
473 ideal compared to titanium.

## 474 **6. Acknowledgements**

475 The research reported in this publication was supported by CRG funding URF/1/2982-01-01  
476 from King Abdullah University of Science and Technology (KAUST) awarded to P.-Y. Hong.

477

478 **7. References**

- 479 [1] J.A. Hargreaves, 2013, Biofloc production systems for  
480 aquaculture, [https://aquaculture.ca.uky.edu/sites/aquaculture.ca.uky.edu/files/srac\\_4503\\_biofloc\\_pro](https://aquaculture.ca.uky.edu/sites/aquaculture.ca.uky.edu/files/srac_4503_biofloc_production_systems_for_aquaculture.pdf)  
481 [duction\\_systems\\_for\\_aquaculture.pdf](https://aquaculture.ca.uky.edu/sites/aquaculture.ca.uky.edu/files/srac_4503_biofloc_production_systems_for_aquaculture.pdf) (Accessed on 23 May 2017)
- 482 [2] A. Sweity, Y. Oren, Z. Ronen, M. Herzberg, The influence of antiscalants on biofouling of RO  
483 membranes in seawater desalination, *Water Res*, 47 (10) (2013) 3389-3398.
- 484 [3] R. Murga, T.S. Forster, E. Brown, J.M. Pruckler, B.S. Fields, R.M. Donlan, Role of biofilms in the  
485 survival of *Legionella pneumophila* in a model potable-water system, *Microbiology*, 147 (Pt 11) (2001)  
486 3121-3126.
- 487 [4] H.Y. Lau, N.J. Ashbolt, The role of biofilms and protozoa in *Legionella* pathogenesis: implications for  
488 drinking water, *J Appl Microbiol*, 107 (2) (2009) 368-378.
- 489 [5] S.E. Coetsier, T.E. Cloete, Biofouling and biocorrosion in industrial water systems, *Crit Rev Microbiol*,  
490 31 (4) (2005) 213-232.
- 491 [6] H.c.A. Videla, *Manual of biocorrosion*, CRC Press, Boca Raton, 1996.
- 492 [7] J. Silhan, C.B. Corfitzen, H.J. Albrechtsen, Effect of temperature and pipe material on biofilm  
493 formation and survival of *Escherichia coli* in used drinking water pipes: a laboratory-based study, *Water*  
494 *Sci Technol*, 54 (3) (2006) 49-56.
- 495 [8] H. Wang, S. Masters, M.A. Edwards, J.O. Falkinham, 3rd, A. Pruden, Effect of disinfectant, water age,  
496 and pipe materials on bacterial and eukaryotic community structure in drinking water biofilm, *Environ*  
497 *Sci Technol*, 48 (3) (2014) 1426-1435.
- 498 [9] I. Douterelo, R.L. Sharpe, J.B. Boxall, Influence of hydraulic regimes on bacterial community structure  
499 and composition in an experimental drinking water distribution system, *Water Res*, 47 (2) (2013) 503-  
500 516.
- 501 [10] J. Yu, D. Kim, T. Lee, Microbial diversity in biofilms on water distribution pipes of different materials,  
502 *Water Sci Technol*, 61 (1) (2010) 163-171.
- 503 [11] P.L. Waines, R. Moate, A.J. Moody, M. Allen, G. Bradley, The effect of material choice on biofilm  
504 formation in a model warm water distribution system, *Biofouling*, 27 (10) (2011) 1161-1174.
- 505 [12] H.J. Jang, Y.J. Choi, J.O. Ka, Effects of diverse water pipe materials on bacterial communities and  
506 water quality in the annular reactor, *J Microbiol Biotechnol*, 21 (2) (2011) 115-123.
- 507 [13] P. Niquette, P. Servais, R. Savoir, Impacts of pipe materials on densities of fixed bacterial biomass in  
508 a drinking water distribution system, *Water Research*, 34 (6) (2000) 1952-1956.
- 509 [14] M.J. Lehtola, I.T. Miettinen, T. Lampola, A. Hirvonen, T. Vartiainen, P.J. Martikainen, Pipeline  
510 materials modify the effectiveness of disinfectants in drinking water distribution systems, *Water*  
511 *Research*, 39 (10) (2005) 1962-1971.
- 512 [15] M.J. Lehtola, K.T. Miettinen, M.M. Keinanen, T.K. Kekki, O. Laine, A. Hirvonen, T. Vartiainen, P.J.  
513 Martikainen, *Microbiology, chemistry and biofilm development in a pilot drinking water distribution*  
514 *system with copper and plastic pipes*, *Water Research*, 38 (17) (2004) 3769-3779.
- 515 [16] H. Tamaki, Y. Sekiguchi, S. Hanada, K. Nakamura, N. Nomura, M. Matsumura, Y. Kamagata,  
516 Comparative analysis of bacterial diversity in freshwater sediment of a shallow eutrophic lake by  
517 molecular and improved cultivation-based techniques, *Appl Environ Microbiol*, 71 (4) (2005) 2162-2169.
- 518 [17] R.I. Amann, W. Ludwig, K.H. Schleifer, Phylogenetic identification and in situ detection of individual  
519 microbial cells without cultivation, *Microbiol Rev*, 59 (1) (1995) 143-169.
- 520 [18] F.M. AlAbbas, C. Williamson, S.M. Bhola, J.R. Spear, D.L. Olson, B. Mishra, A.E. Kakpovbia, Influence  
521 of sulfate reducing bacterial biofilm on corrosion behavior of low-alloy, high-strength steel (API-5L X80),  
522 *Int Biodeter Biodegr*, 78 (2013) 34-42.

523 [19] G. Wegener, V. Krukenberg, D. Riedel, H.E. Tegetmeyer, A. Boetius, Intercellular wiring enables  
524 electron transfer between methanotrophic archaea and bacteria, *Nature*, 526 (7574) (2015) 587-U315.

525 [20] G. Scarascia, T. Wang, P.Y. Hong, Quorum Sensing and the Use of Quorum Quenchers as Natural  
526 Biocides to Inhibit Sulfate-Reducing Bacteria, *Antibiotics (Basel)*, 5 (4) (2016).

527 [21] D. Enning, J. Garrelfs, Corrosion of iron by sulfate-reducing bacteria: new views of an old problem,  
528 *Appl Environ Microbiol*, 80 (4) (2014) 1226-1236.

529 [22] H.C. Flemming, Economical and technical overview, in: E. Heitz, H.C. Flemming, W. Sand (Eds.)  
530 *Microbially influenced corrosion of materials*, Springer-Verlag Berlin Heidelberg, 1996.

531 [23] P. Rodriguez, 1997, Selection of materials for heat  
532 exchangers, [http://www.iaea.org/inis/collection/NCLCollectionStore/ Public/29/000/29000411.pdf](http://www.iaea.org/inis/collection/NCLCollectionStore/Public/29/000/29000411.pdf)  
533 (Accessed on 15 March)

534 [24] H. Cheng, Y. Xie, L.F. Villalobos, L. Song, K.V. Peinemann, S. Nunes, P.Y. Hong, Antibiofilm effect  
535 enhanced by modification of 1,2,3-triazole and palladium nanoparticles on polysulfone membranes, *Sci*  
536 *Rep*, 6 (2016) 24289.

537 [25] R. Förch, H. Schönherr, A.T.A. Jenkins, *Surface Design: Applications in Bioscience and*  
538 *Nanotechnology*, Wiley, 2009.

539 [26] E. Gatza, F. Hammes, E. Prest, Assessing water quality with the BD Accuri™ C6 flow cytometer, in,  
540 *BD Biosciences*, 2013.

541 [27] P.Y. Hong, E. Wheeler, I.K. Cann, R.I. Mackie, Phylogenetic analysis of the fecal microbial community  
542 in herbivorous land and marine iguanas of the Galapagos Islands using 16S rRNA-based pyrosequencing,  
543 *ISME J*, 5 (9) (2011) 1461-1470.

544 [28] R.C. Edgar, B.J. Haas, J.C. Clemente, C. Quince, R. Knight, UCHIME improves sensitivity and speed of  
545 chimera detection, *Bioinformatics*, 27 (16) (2011) 2194-2200.

546 [29] Q. Wang, G.M. Garrity, J.M. Tiedje, J.R. Cole, Naive Bayesian classifier for rapid assignment of rRNA  
547 sequences into the new bacterial taxonomy, *Appl Environ Microbiol*, 73 (16) (2007) 5261-5267.

548 [30] K. Clarke, R. Gorley, PRIMER version 7: user manual/tutorial, PRIMER-E, Plymouth, UK, 296 (2015).

549 [31] J.R. Cole, Q. Wang, J.A. Fish, B. Chai, D.M. McGarrell, Y. Sun, C.T. Brown, A. Porras-Alfaro, C.R.  
550 Kuske, J.M. Tiedje, Ribosomal Database Project: data and tools for high throughput rRNA analysis,  
551 *Nucleic Acids Res*, 42 (Database issue) (2014) D633-642.

552 [32] M. Harb, C.H. Wei, N. Wang, G. Amy, P.Y. Hong, Organic micropollutants in aerobic and anaerobic  
553 membrane bioreactors: Changes in microbial communities and gene expression, *Bioresour Technol*, 218  
554 (2016) 882-891.

555 [33] N. Al-Jassim, M.I. Ansari, M. Harb, P.Y. Hong, Removal of bacterial contaminants and antibiotic  
556 resistance genes by conventional wastewater treatment processes in Saudi Arabia: Is the treated  
557 wastewater safe to reuse for agricultural irrigation?, *Water Research*, 73 (2015) 277-290.

558 [34] W.G. Characklis, G.A. McFeters, K.C. Marshall, Physiological ecology in biofilm systems, in: W.G.  
559 Characklis, K.C. Marshall (Eds.) *Biofilms*, John Wiley & Sons, New York, 1990, pp. 341-394.

560 [35] M. Fletcher, G.I. Loeb, Influence of substratum characteristics on the attachment of a marine  
561 pseudomonad to solid surfaces, *Appl Environ Microbiol*, 37 (1) (1979) 67-72.

562 [36] J.H. Pringle, M. Fletcher, Influence of substratum wettability on attachment of freshwater bacteria  
563 to solid surfaces, *Appl Environ Microbiol*, 45 (3) (1983) 811-817.

564 [37] B. Bending, H.H. Rijnaarts, K. Altendorf, A.J. Zehnder, Physicochemical cell surface and adhesive  
565 properties of coryneform bacteria related to the presence and chain length of mycolic acids, *Appl*  
566 *Environ Microbiol*, 59 (11) (1993) 3973-3977.

567 [38] J. Wingender, H.C. Flemming, Contamination potential of drinking water distribution network  
568 biofilms, *Water Sci Technol*, 49 (11-12) (2004) 277-286.

569 [39] C.M. Pang, P. Hong, H. Guo, W.T. Liu, Biofilm formation characteristics of bacterial isolates retrieved  
570 from a reverse osmosis membrane, *Environ Sci Technol*, 39 (19) (2005) 7541-7550.



571 [40] J. Rogers, A.B. Dowsett, P.J. Dennis, J.V. Lee, C.W. Keevil, Influence of Plumbing Materials on Biofilm  
572 Formation and Growth of *Legionella pneumophila* in Potable Water Systems, *Appl Environ Microbiol*, 60  
573 (6) (1994) 1842-1851.

574 [41] X. Hu, K.G. Neoh, J. Zhang, E.-T. Kang, Bacterial and osteoblast behavior on titanium, cobalt-  
575 chromium alloy and stainless steel treated with alkali and heat: A comparative study for potential  
576 orthopedic applications, *Journal of Colloid and Interface Science*, 417 (2014) 410-419.

577 [42] E. Velasco-Ortega, A. Jos, A.M. Camean, J. Pato-Mourelo, J.J. Segura-Egea, In vitro evaluation of  
578 cytotoxicity and genotoxicity of a commercial titanium alloy for dental implantology, *Mutat Res*, 702 (1)  
579 (2010) 17-23.

580 [43] D. Xu, T. Gu, Carbon source starvation triggered more aggressive corrosion against carbon steel by  
581 the *Desulfovibrio vulgaris* biofilm, *Int Biodeter Biodegr*, 91 (2014) 74-81.

582 [44] P. Zhang, D. Xu, Y. Li, K. Yang, T. Gu, Electron mediators accelerate the microbiologically influenced  
583 corrosion of 304 stainless steel by the *Desulfovibrio vulgaris* biofilm, *Bioelectrochemistry*, 101 (2015) 14-  
584 21.

585 [45] B. Anandkumar, R.P. George, S. Maruthamuthu, N. Palaniswamy, R.K. Dayal, Corrosion behavior of  
586 SRB *Desulfovibrio propionicus* isolated from an Indian petroleum refinery on mild steel, *Materials and*  
587 *Corrosion*, 63 (4) (2012) 355-362.

588 [46] N. LaBarge, Y.D. Yilmazel, P.Y. Hong, B.E. Logan, Effect of pre-acclimation of granular activated  
589 carbon on microbial electrolysis cell startup and performance, *Bioelectrochemistry*, 113 (2017) 20-25.

590 [47] N. LaBarge, Y. Ye, K.-Y. Kim, Y.D. Yilmazel, P.E. Saikaly, P.-Y. Hong, B.E. Logan, Impact of acclimation  
591 methods on microbial communities and performance of anaerobic fluidized bed membrane bioreactors,  
592 *Environmental Science: Water Research & Technology*, 2 (6) (2016) 1041-1048.

593 [48] K. Rabaey, N. Boon, M. Hofte, W. Verstraete, Microbial phenazine production enhances electron  
594 transfer in biofuel cells, *Environ Sci Technol*, 39 (9) (2005) 3401-3408.

595 [49] K. Rabaey, N. Boon, S.D. Siciliano, M. Verhaege, W. Verstraete, Biofuel cells select for microbial  
596 consortia that self-mediate electron transfer, *Appl Environ Microbiol*, 70 (9) (2004) 5373-5382.

597 [50] C.K. Stover, X.Q. Pham, A.L. Erwin, S.D. Mizoguchi, P. Warrenner, M.J. Hickey, F.S. Brinkman, W.O.  
598 Hufnagle, D.J. Kowalik, M. Lagrou, R.L. Garber, L. Goltry, E. Tolentino, S. Westbrook-Wadman, Y. Yuan,  
599 L.L. Brody, S.N. Coulter, K.R. Folger, A. Kas, K. Larbig, R. Lim, K. Smith, D. Spencer, G.K. Wong, Z. Wu, I.T.  
600 Paulsen, J. Reizer, M.H. Saier, R.E. Hancock, S. Lory, M.V. Olson, Complete genome sequence of  
601 *Pseudomonas aeruginosa* PAO1, an opportunistic pathogen, *Nature*, 406 (6799) (2000) 959-964.

602 [51] P.Y. Hong, N. Moosa, J. Mink, Dynamics of microbial communities in an integrated ultrafiltration-  
603 reverse osmosis desalination pilot plant located at the Arabian Gulf, *Desalin Water Treat*, 57 (35) (2016)  
604 16310-16323.

605 [52] TotalMateria, 2005, Physical properties of titanium and its  
606 alloys, <http://www.totalmateria.com/Article122.htm> (Accessed on 3 October 2017)

607 [53] L.C. Simoes, M. Simoes, R. Oliveira, M.J. Vieira, Potential of the adhesion of bacteria isolated from  
608 drinking water to materials, *J Basic Microbiol*, 47 (2) (2007) 174-183.

609 [54] P.M. Erwin, M.C. Pineda, N. Webster, X. Turon, S. Lopez-Legentil, Down under the tunic: bacterial  
610 biodiversity hotspots and widespread ammonia-oxidizing archaea in coral reef ascidians, *ISME J*, 8 (3)  
611 (2014) 575-588.

612 [55] R. Seshadri, I.T. Paulsen, J.A. Eisen, T.D. Read, K.E. Nelson, W.C. Nelson, N.L. Ward, H. Tettelin, T.M.  
613 Davidsen, M.J. Beanan, R.T. Deboy, S.C. Daugherty, L.M. Brinkac, R. Madupu, R.J. Dodson, H.M. Khouri,  
614 K.H. Lee, H.A. Carty, D. Scanlan, R.A. Heinzen, H.A. Thompson, J.E. Samuel, C.M. Fraser, J.F. Heidelberg,  
615 Complete genome sequence of the Q-fever pathogen *Coxiella burnetii*, *Proc Natl Acad Sci U S A*, 100 (9)  
616 (2003) 5455-5460.

617 [56] S. Lucker, D. Steger, K.U. Kjeldsen, B.J. MacGregor, M. Wagner, A. Loy, Improved 16S rRNA-targeted  
618 probe set for analysis of sulfate-reducing bacteria by fluorescence in situ hybridization, *J Microbiol*  
619 *Methods*, 69 (3) (2007) 523-528.

620 [57] G. Muyzer, E.C. de Waal, A.G. Uitterlinden, Profiling of complex microbial populations by denaturing  
621 gradient gel electrophoresis analysis of polymerase chain reaction-amplified genes coding for 16S rRNA,  
622 *Appl Environ Microbiol*, 59 (3) (1993) 695-700.

623 [58] A. Loy, A. Lehner, N. Lee, J. Adamczyk, H. Meier, J. Ernst, K.H. Schleifer, M. Wagner, Oligonucleotide  
624 microarray for 16S rRNA gene-based detection of all recognized lineages of sulfate-reducing prokaryotes  
625 in the environment, *Appl Environ Microbiol*, 68 (10) (2002) 5064-5081.

626 [59] M.J. McConnell, A. Perez-Ordóñez, P. Perez-Romero, R. Valencia, J.A. Lepe, I. Vázquez-Barba, J.  
627 Pachon, Quantitative real-time PCR for detection of *Acinetobacter baumannii* colonization in the  
628 hospital environment, *J Clin Microbiol*, 50 (4) (2012) 1412-1414.

629

630

631 **Table 1.** Primers used for quantitative PCR.

<b>Target</b>	<b>Primer name</b>	<b>Sequences (5'-3')</b>	<b>Reference</b>
Desulfobacteraceae (16S rRNA genes)	DSBAC357F	GTGAGGAATTTTGC GCAATGG	[56]
	519R	GWATTACCGCGGCKGCTG	[57]
Desulfobulbaceae (16S rRNA genes)	519F	CAGCMGCCGCGGTAATWC	[57]
	DSB706R	ACCGGTATTCTCCCGAT	[58]
<i>Acinetobacter baumannii</i> ( <i>ompA</i> gene)	<i>ompA</i> -F	TCTTGGTGGTCACTTGAAGC	[59]
	<i>ompA</i> -R	ACTCTTGTGGTTGTGGAGCA	

632

633

634 **Table 2.** Surface characteristics of the tested materials.

	<b>Average root mean square, RMS, of surface (n = 3) ± standard deviation</b>	<b>Average liquid-solid contact angle (n = 6) ± standard deviation</b>
HDPE	0.24 ± 0.18 <sup>a</sup>	63.9° ± 1.8°
Polycarbonate	0.53 ± 0.20 <sup>b</sup>	61.6° ± 1.7°
Titanium	0.19 ± 0.11 <sup>a</sup>	80.2° ± 1.5°
Stainless steel SS316	0.19 ± 0.06 <sup>a</sup>	75.6° ± 0.9°

635 a, b Homogenous subgroups by two-tailed t-test method with a significance level of 0.10

636

637 **Table 3.** ANOSIM R statistic values and p-values between the **(A)** different materials, and **(B)** sampling  
 638 months. Values in bold refer to significant differences between the sample pairs at the 90% confidence  
 639 level.

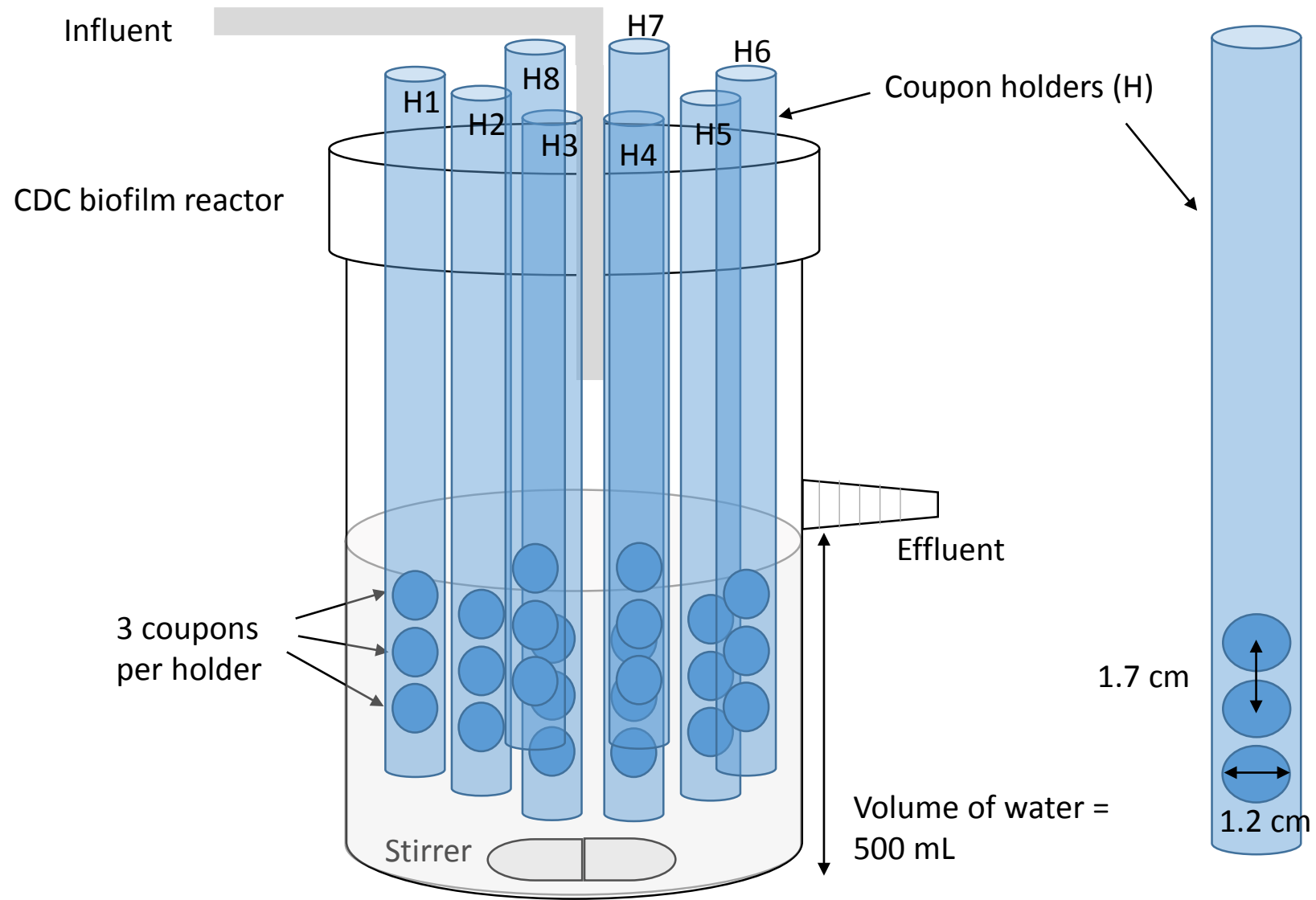
640  
 641

<b>A.</b>	Seawater	HDPE	Polycarbonate	Titanium	SS316
Seawater		<b>0.382</b> (p = <b>0.008</b> )	<b>0.357</b> (p = <b>0.011</b> )	<b>0.436</b> (p = <b>0.016</b> )	<b>0.171</b> (p = <b>0.065</b> )
HDPE			-0.139 (p = 0.967)	-0.128 (p = 0.133)	<b>0.163</b> (p = <b>0.054</b> )
Polycarbonate				0.149 (p = 0.108)	<b>0.133</b> (p = <b>0.100</b> )
Titanium					0.037 (p = 0.305)
SS316					

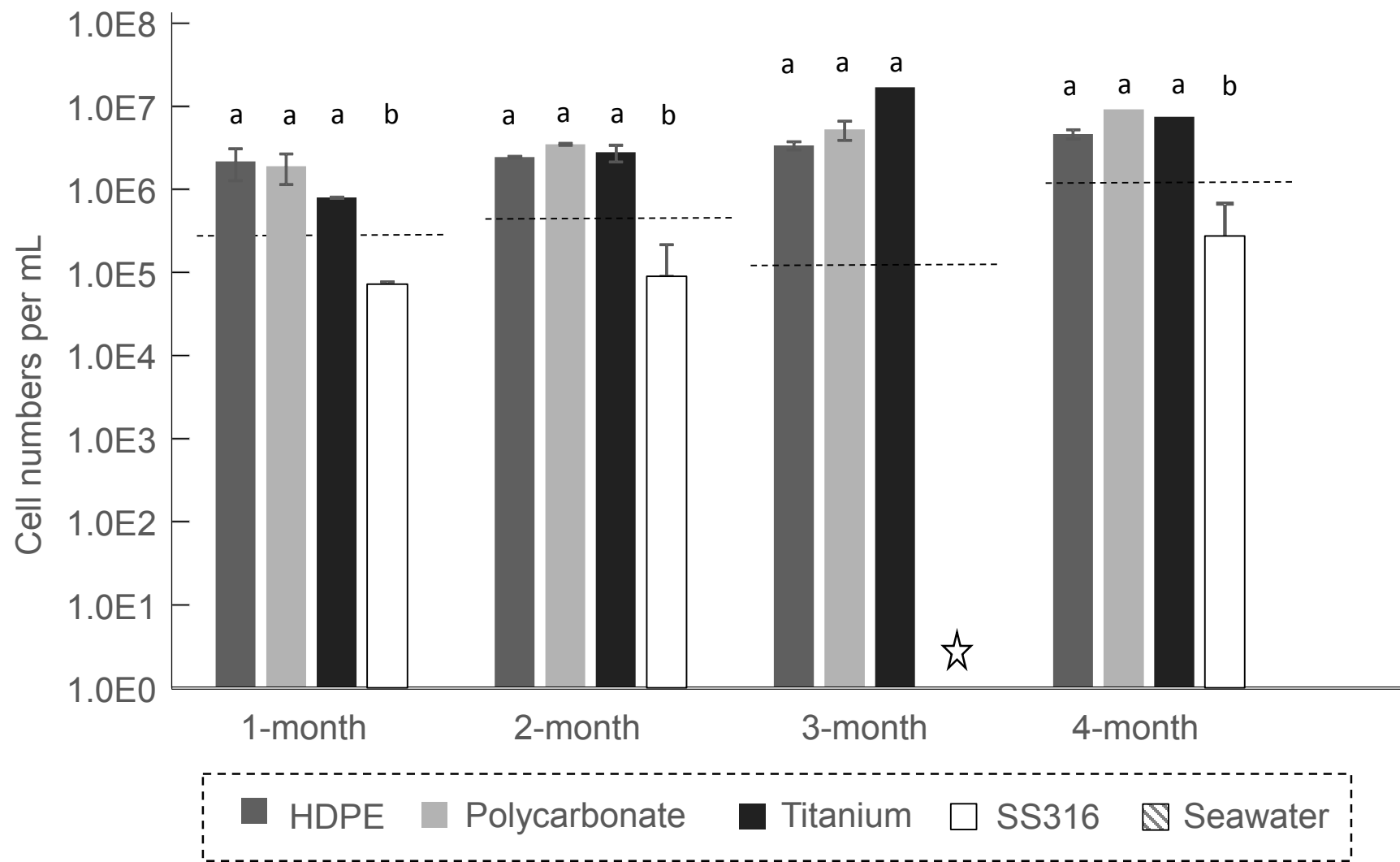
642  
 643

<b>B.</b>	1-month	2-month	3-month	4-month
1-month		0.041 (p = 0.309)	-0.005 (p = 0.485)	0.125 (p = 0.115)
2-month			0.058 (p = 0.228)	0.087 (p = 0.146)
3-month				-0.009 (p = 0.404)
4-month				

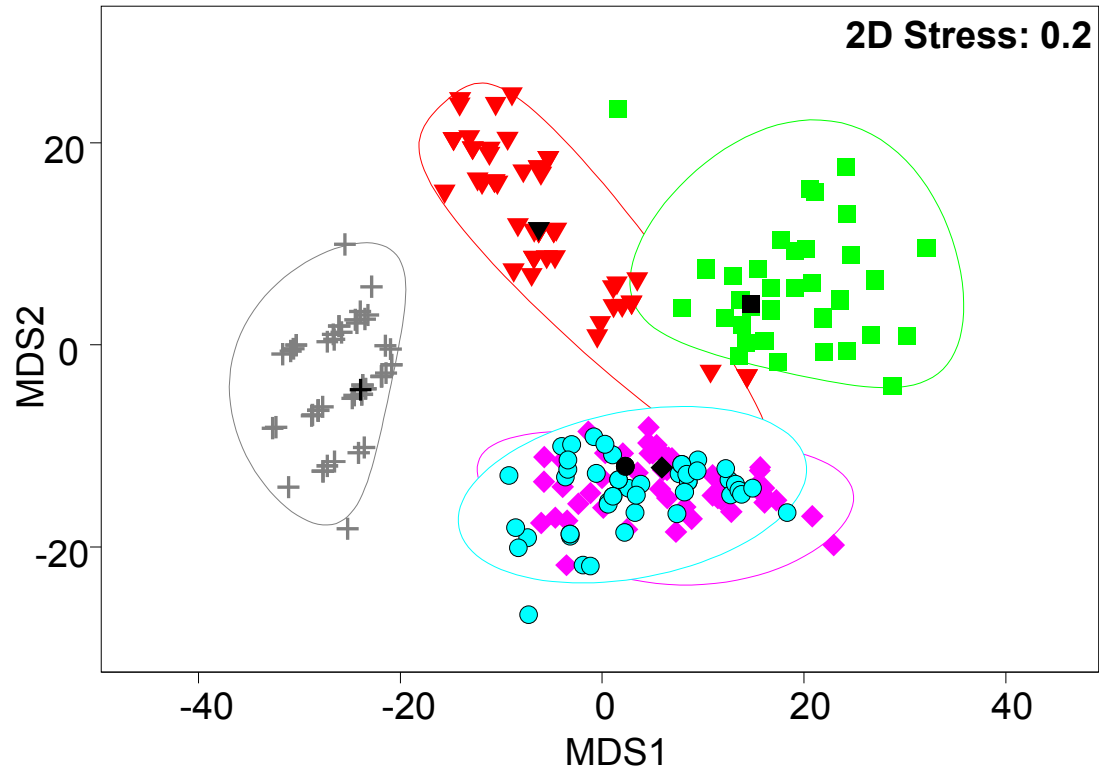
644  
 645  
 646  
 647



**Figure 1.** Illustration of the CDC biofilm reactor.



**Figure 2.** Enumeration of total cell counts attached to different types of materials over a duration of four months. The star denotes no measurements obtained for that sampling month for SS316 due to sampling error. a, b denote homogenous subgroups by two-tailed t-test method with a significance level of 0.10. Dash lines correspond to the cell numbers per mL of seawater at that month. Star denotes no measurements were obtained for that sampling month for stainless steel.

**(A)****Material**

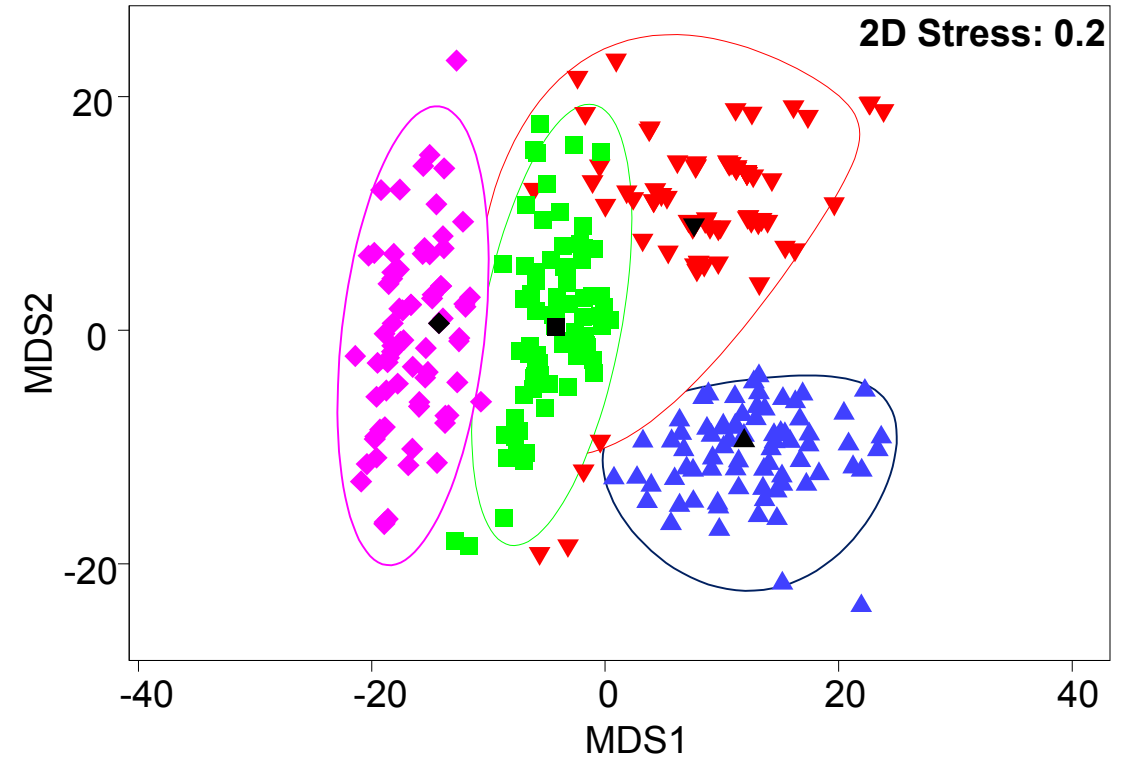
▼ SS316

◆ HDPE

+ Seawater

■ Titanium

● Polycarbonate

**(B)****Time**

▲ 1-month

▼ 2-month

■ 3-month

◆ 4-month

**Figure 3.** Bootstrapped metric multidimensional scaling (MDS) plots of microbial communities in relation to **(A)** the type of material and **(B)** the temporal effect.



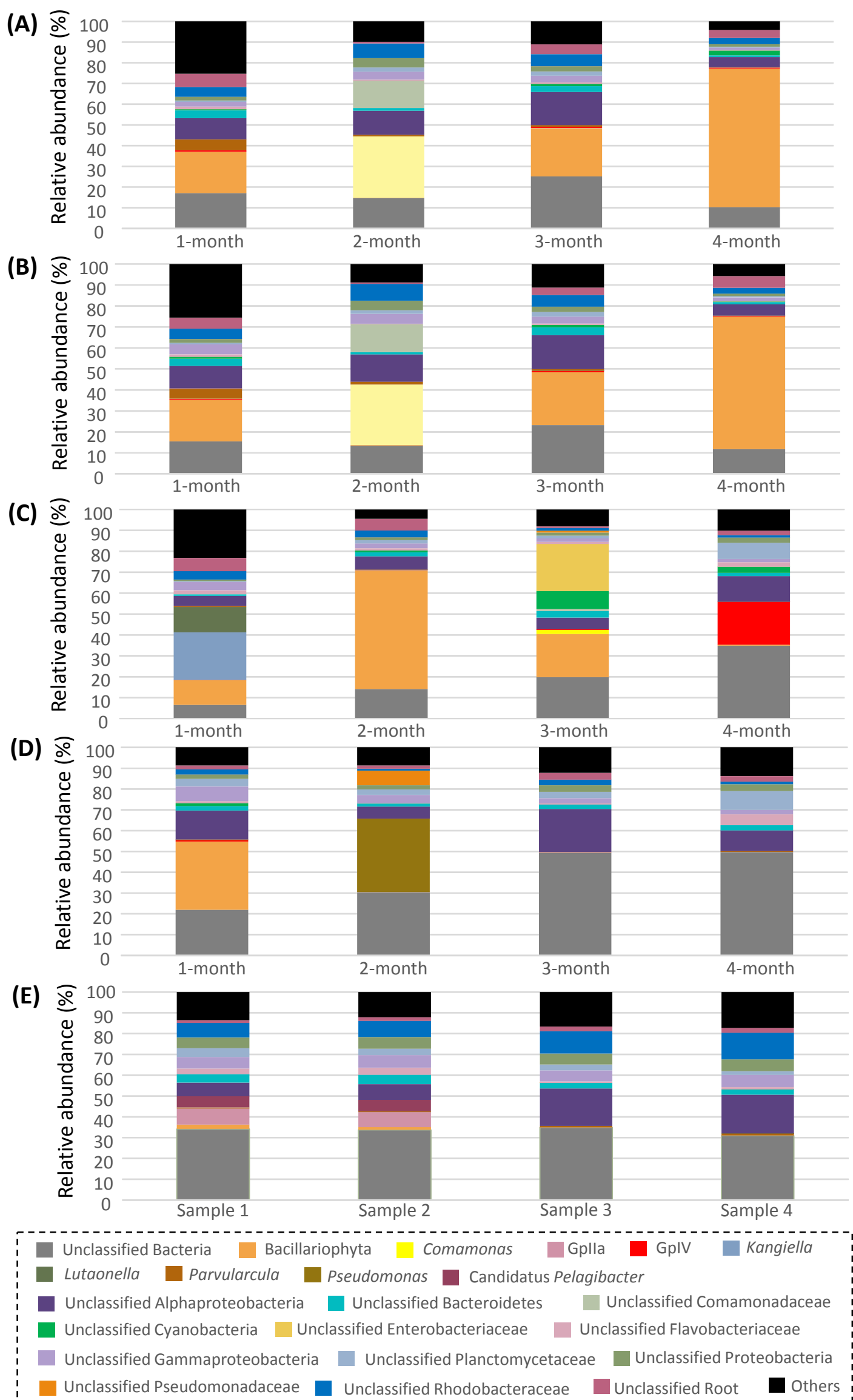
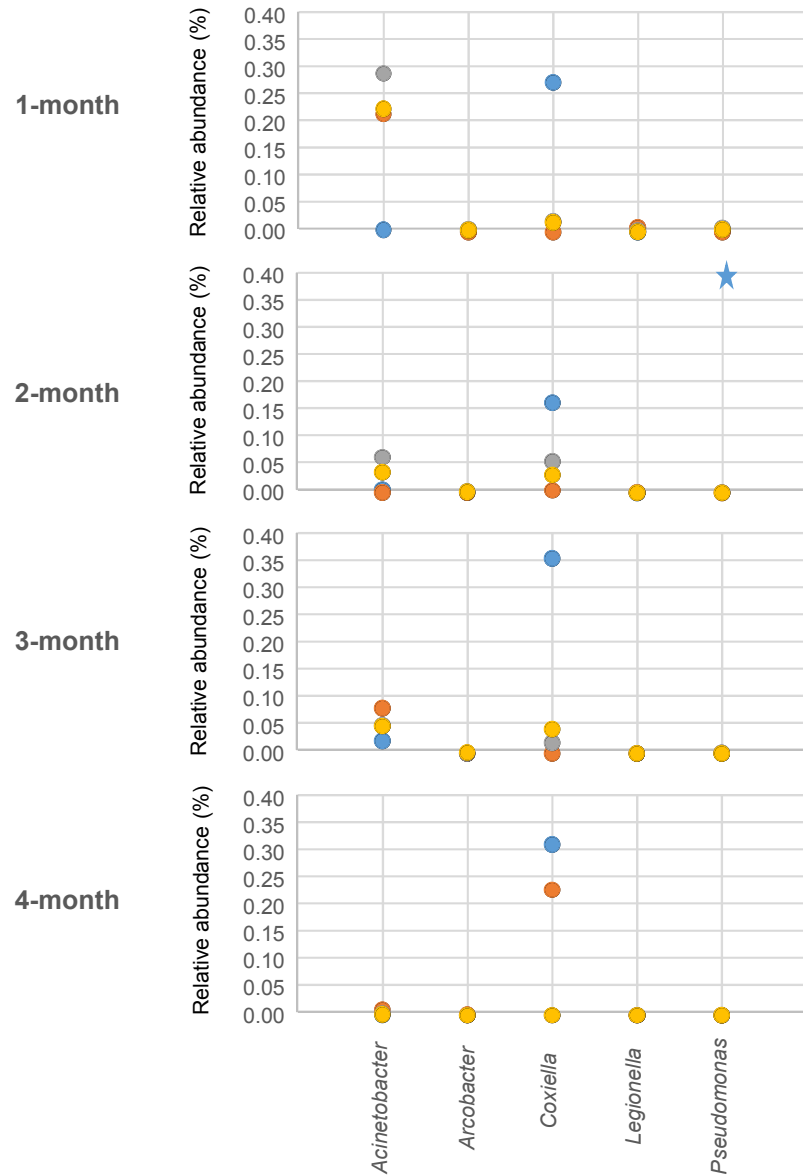


**Figure 4.** The relative abundances obtained by high-throughput sequencing, representing the predominant microbial taxa attached to (A) HDPE, (B) polycarbonate, (C) titanium, (D) SS316, and in (E) seawater

**(A)** ● SS316 ● Titanium ● HDPE ● Polycarbonate



**(B)** ● SS316 ● Titanium ● HDPE ● Polycarbonate

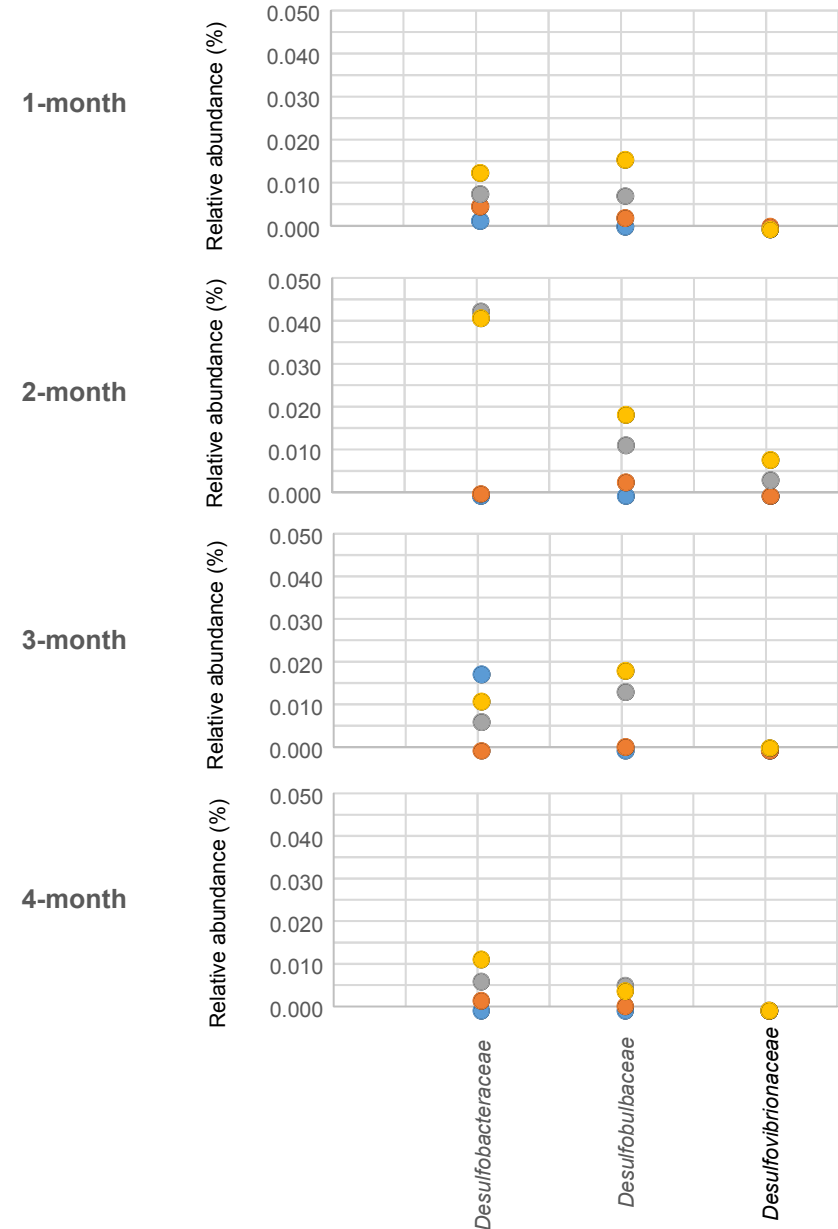


**Figure 5.** The relative abundances obtained by high-throughput sequencing representing **(A)** genera associated with opportunistic pathogens, and **(B)** selected sulfate-reducing bacteria identified at the family taxonomical level. The star denotes that the relative abundance of *Pseudomonas* was exceedingly high for SS316 at the 2-month sampling event and fell out of the range shown on the y-axis.

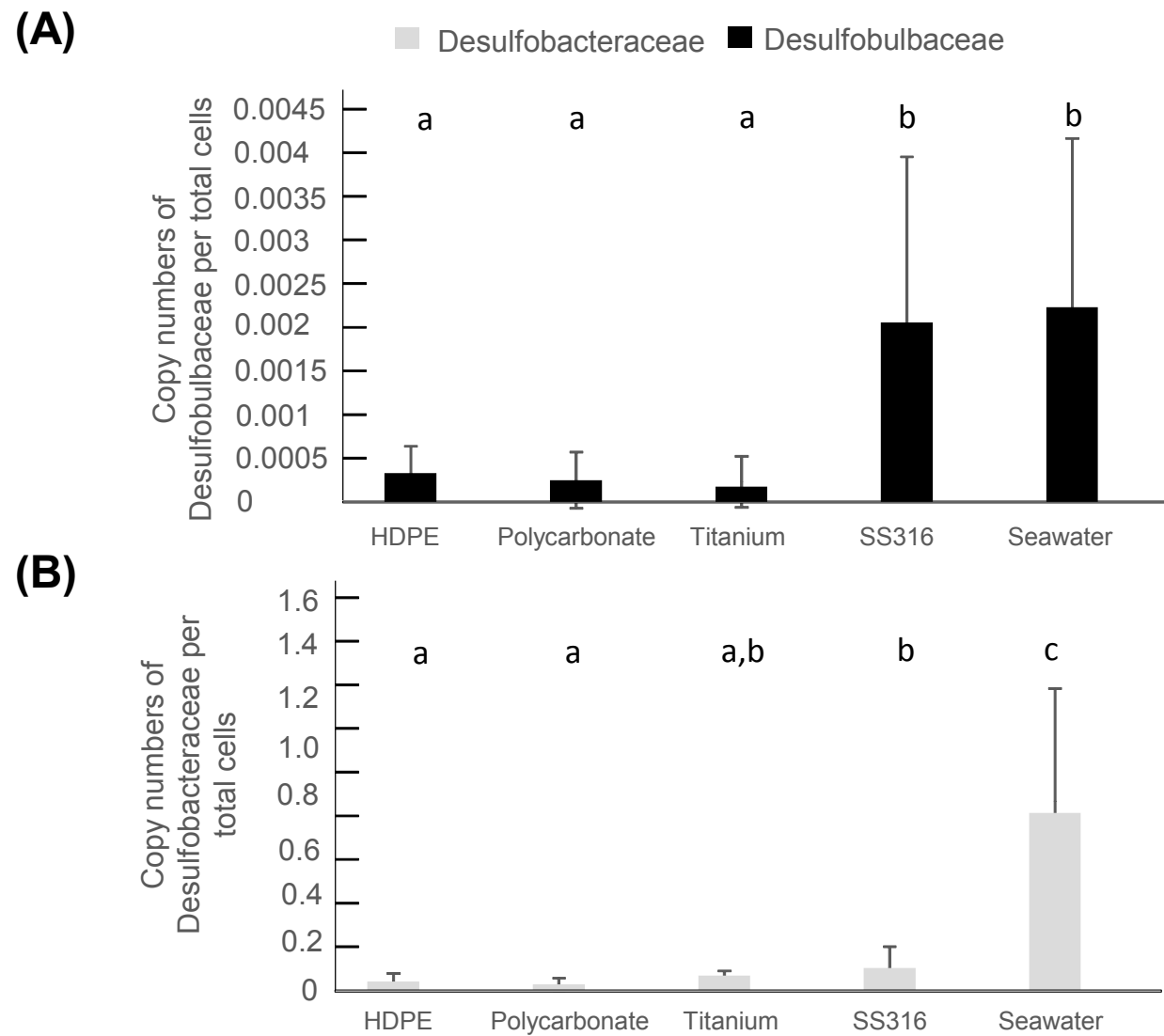


**Figure 6.** Copy numbers of 16S rRNA genes representative of Desulfobacteraceae and Desulfobulbaceae obtained by quantitative PCR and normalized against total cells. Both Desulfobacteraceae and Desulfobulbaceae comprise genera representative of sulfate-reducing bacteria. a, b, c denote homogenous subgroups by two-tailed t-test method with a significance level of 0.10.